AEDC-TR-83-64
C2

# Optical Constant Determination of Thin Films Condensed on Transmitting and Reflecting Substrates

Property of U. S. Air Force
AEDC LIBRARY
F40600-81-C-0004

K. F. Palmer
and
M. Z. Williams
Westminster College
Fulton, MO

May 1984

Final Report for Period October 1, 1982 to September 30, 1983

TECHNICAL REPORTS
FILE COPY

Approved for public release; distribution unlimited.

ARNOLD ENGINEERING DEVELOPMENT CENTER
ARNOLD AIR FORCE STATION, TENNESSEE
AIR FORCE SYSTEMS COMMAND
UNITED STATES AIR FORCE

## NOTICES

When U. S. Government drawings, specifications, or other data are used for any purpose other than a definitely related Government procurement operation, the Government thereby incurs no responsibility nor any obligation whatsoever, and the fact that the government may have formulated, furnished, or in any way supplied the said drawings, specifications, or other data, is not to be regarded by implication or otherwise, or in any manner licensing the holder or any other person or corporation, or conveying any rights or permission to manufacture, use, or sell any patented invention that may in any way be related thereto.

Qualified users may obtain copies of this report from the Defense Technical Information Center.

References to named commercial products in this report are not to be considered in any sense as an endorsement of the product by the United States Air Force or the Government.

This report has been reviewed by the Office of Public Affairs (PA) and is releasable to the National Technical Information Service (NTIS). At NTIS, it will be available to the general public, including foreign nations.

**APPROVAL STATEMENT**

This report has been reviewed and approved.

KENNETH H. LENERS, Captain, USAF
Directorate of Technology
Deputy for Operations

Approved for publication:

FOR THE COMMANDER

MARION L. LASTER
Director of Technology
Deputy for Operations

UNCLASSIFIED

SECURITY CLASSIFICATION OF THIS PAGE (When Data Entered)

# REPORT DOCUMENTATION PAGE

READ INSTRUCTIONS BEFORE COMPLETING FORM

1. REPORT NUMBER: AEDC-TR-83-64

2. GOVT ACCESSION NO.

3. RECIPIENT'S CATALOG NUMBER

4. TITLE (and Subtitle): OPTICAL CONSTANT DETERMINATION OF THIN FILMS CONDENSED ON TRANSMITTING AND REFLECTING SUBSTRATES

5. TYPE OF REPORT & PERIOD COVERED: Final Report for Period Oct 1, 1982 to Sept. 30, 1983

6. PERFORMING ORG. REPORT NUMBER


7. AUTHOR(s): K. F. Palmer and M. Z. Williams, Westminister College, Fulton, MO


8. CONTRACT OR GRANT NUMBER(s)

9. PERFORMING ORGANIZATION NAME AND ADDRESS: Arnold Engineering Development Center/DOT, Air Force Systems Command, Arnold Air Force Station, Tennessee 37389

10. PROGRAM ELEMENT, PROJECT, TASK AREA & WORK UNIT NUMBERS: 65807F

11. CONTROLLING OFFICE NAME AND ADDRESS: Arnold Engineering Development Center/DOS, Air Force Systems Command, Arnold Air Force Station, Tennessee 37389

12. REPORT DATE: May 1984

13. NUMBER OF PAGES: 57

14. MONITORING AGENCY NAME & ADDRESS (if different from Controlling Office)

15. SECURITY CLASS. (of this report): Unclassified

15a. DECLASSIFICATION/DOWNGRADING SCHEDULE: N/A

16. DISTRIBUTION STATEMENT (of this Report)

Approved for public release; distribution unlimited.

17. DISTRIBUTION STATEMENT (of the abstract entered in Block 20, if different from Report)

18. SUPPLEMENTARY NOTES

Available in Defense Technical Information Center (DTIC).

19. KEY WORDS (Continue on reverse side if necessary and identify by block number)

| | |
|---|---|
| reflectance | substrates |
| optical properties | dielectric film |
| thin film | germanium |
| transmittance | computer programs |

20. ABSTRACT (Continue on reverse side if necessary and identify by block number)


In this report, a new subtractive Kramers-Kronig (SKK) computer program is described which can obtain accurate optical constants of a uniform thin film on a thick substrate using only the transmittance measurements of a single-film thickness. Preliminary results from existing AEDC data show that the optical properties of a dielectric film may depend, to a small degree, upon the thickness of the film. This effect seems to be more noticeable in films containing molecules, such as $H_2O$ and $NH_3$, which readily form hydrogen bonds.


DD FORM 1 JAN 73 1473 EDITION OF 1 NOV 65 IS OBSOLETE

UNCLASSIFIED

SECURITY CLASSIFICATION OF THIS PAGE (When Data Entered)

20. Concluded

Also described are two methods for extracting the optical constants of a dielectric thin film from measurements of the reflectance of a beam incident in a vacuum upon a film layer on a metal substrate. In one method, the dependence is observed of the reflectances of several thicknesses of the same film material upon its thickness. This method contains the assumption that the optical properties of a film material do not vary with changes in film thickness.

The second method does not depend on this assumption. It uses the reflectance spectrum of a single-film thickness to compute the optical constants of the film from a dispersion relation.

## PREFACE

Work reported herein was sponsored by the Arnold Engineering Development Center (AEDC), Directorate of Technology (DOT). The work was done by Dr. Kent Palmer and Dr. M. Z. Williams of Westminster College in Fulton, Missouri who were under subcontract to Calspan Field Services, Inc., AEDC Division, operating contractor for aerospace flight dynamics testing at AEDC, AFSC, Arnold Air Force Station, Tennessee. This work was accomplished under project numbers D218PW and D641PW. The Calspan project monitor was B. E. Wood, and the Air Force Project Manager was Capt. K. H. Leners. The manuscript was submitted for publication on December 5, 1983.

# CONTENTS

Page

1.0 INTRODUCTION ..... 5
1.1 ANALYSIS OF TRANSMITTANCE MEASUREMENTS OF THIN FILMS ..... 5
1.2 ANALYSIS OF REFLECTANCE MEASUREMENTS OF THIN FILMS ..... 6
2.0 EXTRACTION OF THE OPTICAL CONSTANTS OF A THIN FILM FROM TRANSMISSION MEASUREMENTS OF A SINGLE- FILM THICKNESS ..... 7
2.1 THEORY ..... 7
2.1.1 Determination of Phase $\phi$ of $\hat{t}$ ..... 10
2.1.2 Derivation of the SKK Relation ..... 11
2.1.3 Determination of the Integer m in Eq. (12) ..... 12
2.1.4 Estimation of the Complex Index of Refraction $\hat{n}$ of the Film ..... 13
2.1.5 Extrapolations of the Data ..... 14
2.2 COMPUTER PROGRAM SKKTRANS ..... 17
2.2.1 Program Segment KAMKON ..... 18
2.2.2 Program Segment ANALYSIS ..... 18
2.2.2.1 Selection of the "Best" Pair of Optical Constants ..... 18
2.3 PRELIMINARY RESULTS FROM SKKTRANS ..... 19
2.3.1 Test of the SKK and the Interpolation Algorithms ..... 20
2.3.2 Variation of $\phi(\nu_0) + 2m\pi$ with Film Thickness ..... 22
2.3.3 Changes in the n- and k-Spectra as a Function of Film Thickness $d_1$ ..... 25
2.4 USING PROGRAM SKKTRANS ..... 28
2.4.1 Program Parameters ..... 28
2.4.2 Spectra with Overlapping Bands ..... 29
3.0 DETERMINATION OF THE OPTICAL CONSTANTS OF A DIELECTRIC THIN FILM ON A METAL SUBSTRATE FROM REFLECTANCE MEASUREMENTS OF A SINGLE-FILM THICKNESS ..... 29
3.1 Theory ..... 30
3.1.1 Absolute Reflectance $R_{012}$ ..... 32
3.1.2 Relative Reflectance R ..... 32
3.1.3 Absolute Reflectance $R_{02}$ of the Vacuum-Metal Interface ..... 32
3.1.4 Evaluation of $\hat{n}_2$ from $R_{02}$ ..... 33

Page

3.1.5 Multiple-Film Thickness Method ..... 35
3.1.6 Single-Film Thickness Method ..... 35
3.1.7 Derivation of the Kramers-Kronig (KK) Dispersion Relations for $\hat{r}_{012}$ ..... 36
3.1.7.1 Extension of Optical Quantities into the Complex $\hat{\nu}$-Plane ..... 36
3.1.7.2 Poles and Zeros of $\hat{r}_{012}(\hat{\nu})$ ..... 36
3.1.7.3 Evaluation of $\oint_C \hat{S}(\hat{\nu})d\hat{\nu}/(\hat{\nu}^2 - \nu^2) = 0$ ..... 38
3.1.7.4 Case of $S(\hat{\nu}) = \ln \hat{r}_{012}(\hat{\nu})$ ..... 41
3.1.7.5 Kramers-Kronig Dispersion Relation for $\phi(\nu)$ ..... 44
3.1.8 Subtractive Kramers-Kronig (SKK) Relation for $\phi(\nu)$ ..... 45
3.2 LOCATION OF THE ZEROS OF $\hat{r}_{012}$ ..... 46
3.2.1 Finite Number of Zeros ..... 46
3.2.2 Approximate Values of $\hat{n}_1$ and $\hat{n}_2$ ..... 47
3.2.3 Test of an Iterative Method to Find the Zeros ..... 48
3.3 COMPUTER PROGRAM SKKREFL ..... 50
4.0 MULTIPLE-FILM THICKNESS METHOD: Program RENLIN ..... 50
5.0 CONCLUSIONS ..... 57
REFERENCES ..... 52

## ILLUSTRATIONS

Figure | Page

1. Geometry Depicting Analytical Model for a Thin Film Formed Upon a Thick Substrate ..... 8
2. Refractive and Absorption Indices of an Absorption Having a Cauchy (Lorentzian) Bandshape ..... 15
3. Refractive Index of Solid $CO_2$ on 20-K Germanium ..... 21
4. Absorption Index of Solid $CO_2$ on 20-K Germanium ..... 23
5. Plot of Phase Shift $\phi = \phi_0 + 2m\pi$ at $\nu_0 = 2144\ cm^{-1}$ of $N_2/CO_2$ (74.7%/25.3%) Films at 20-K Germanium ..... 24
6. Refractive Index of Solid $N_2/CO_2$ Mixture (74.7%/25.3%) on 20-K Germanium Computed at Several Thicknesses ..... 26
7. Absorption Index of Solid $N_2/CO_2$ Mixture (74.7%/25.3%) on 20-K Germanium Computed at Several Thicknesses ..... 27
8. Geometry Depicting the Analytical Model for a Thin Film Sandwiched Between Two Semi-Infinite Media ..... 31
9. Path C of Contour Integration $\oint_C \hat{S}(\hat{\nu})d\hat{\nu}/(\hat{\nu}^2 - \nu^2)$ ..... 38

# 1.0 INTRODUCTION

The effects of material outgassing are of continuing concern to satellite designers since they are being asked to extend the usable lifetime of space satellites. The lifetime is most often directly related to contamination of spacecraft critical surfaces. During the past few years considerable progress has been made at AEDC in the area of contamination and optical property measurements. Both experimental and analytical efforts have been made in the determination of optical properties used in characterizing contaminants.

The basic property required for determining optical contamination effects is the complex refractive index $\hat{n}(\nu) = n(\nu) + ik(\nu)$, where $n(\nu)$ is commonly referred to as the real part of the refractive index and k is the absorption index of the contaminant film. Knowing $n(\nu)$ and $k(\nu)$, one can calculate the transmittance or reflectance of any contaminant film substrate for a given film thickness through the use of Fresnel's equations within a mathematical model. Conversely, n and k can be theoretically calculated from a film-substrate combination provided transmittance data for two film thicknesses can be obtained and used within a mathematical model such that there are two equations involving n and k, the two unknowns. This was the technique utilized in determining n and k from transmittance measurements in Refs. 1 through 4.

In measurements of contamination of any facility, a method for determining effects of contaminant as a function of contaminant thickness is required. Since most problems are associated with films a few microns thick or less, conventional techniques for thickness measurement do not apply. However, thin film optical interference provides an excellent technique for determining thin film thickness, e.g., film thickness from 0.25 to 25 $\mu$m. This requires knowledge of the refractive index at some known wavelength. After having found the refractive index and thickness, there are techniques available for determining the complex refractive indices (n's and k's) of the film. The subject of this report is the development of the mathematical models and computer programs required for determination of n and k from transmittance and reflectance experimental data. Computer programs TRNLIN and SKKTRANS are used for analyzing transmittance data of multiple films and a single film, respectively, whereas RENLIN and SKKRFL utilize reflectance data of multiple films and a single film, respectively.

## 1.1 ANALYSIS OF TRANSMITTANCE MEASUREMENTS OF THIN FILMS

When a beam of monochromatic light is incident upon a thin film deposited on a thick substrate, a reduction in the intensities of the transmitted and reflected beams is expected, as well as phase shifts of the latter two beams from that of the incident beam. At a given wavenumber, $\nu$, the reduction of beam intensities and the phase shifts depend, in part, upon the values of the film refractive index, $n(\nu)$, and its absorption index, $k(\nu)$.

In one method of obtaining the complex refractive index $\hat{n}(\nu) = n(\nu) + ik(\nu)$ of dielectric films, the differences that changes in film thickness make upon the absolute transmittance are observed (Refs. 1 through 4). (The circumflex denotes a complex quantity.) Because only the transmittance is observed, at least two separate pairs of transmittance and thickness measurements are necessary at each wavenumber, $\nu$, because two optical parameters of the film are sought, $n(\nu)$ and $k(\nu)$.

If, however, the phase shifts corresponding to each transmittance value are known, then the transmittance measurement for only one value of the film thickness is needed to find $n(\nu)$ and $k(\nu)$. Also, the assumption upon which the method is based, that the optical properties of a dielectric film are independent of film thickness, is not required.

Section 2.0 describes a method for finding the optical constants from the transmittance spectrum of a single thin film, even when one cannot directly measure the change of phase spectrum. In it is discussed the pertinent theory and the computer algorithms derived from them. Also shown are the results of a preliminary investigation of some existing AEDC transmittance data for 20-K cryofilms.

## 1.2 ANALYSIS OF REFLECTANCE MEASUREMENTS OF THIN FILMS

In this report, two methods are described for using reflectance measurements to find the optical constants of a thin dielectric film having parallel plane interfaces with a vacuum and a thick metal substrate. The reflectance is that of an infrared (IR) beam of radiation that is nearly normally incident upon the film in the vacuum.

In the more common of the two methods, at a given wavenumber, the variance in the reflectance corresponding to changes in film thickness is observed. This procedure is called the "multiple-film thickness method." If the reflectance measurements of at least two thicknesses of the same film material are available, the experimenter can compute the complex index of refraction, $\hat{n} = n + ik$, from a least-squares algorithm.

At the heart of this method is the assumption that the optical constants n and k of a film material are independent of the film thickness, at least over the experimental range of thickness values. This assumption does not hold at all for very thin metallic films (Ref. 5), and the slight dependence of n and k of $N_2/CO_2$ films on 20-K germanium (Ge) upon their thickness (Section 2.3.3) is demonstrated.

The second method finds n and k of a film from reflectance measurements of a single-film thickness, and the assumed independence of n or k upon the film thickness is not necessary. With this method, one calculates the optical constants from a dispersion relation relating the modulus of the complex reflection coefficient with its phase.

This "single-film thickness method" has worked successfully when applied to the reflectance measurements of a dielectric film deposited on a medium whose modulus of the complex index was lower than that of the film (Ref. 6), but no one has fully tested its applicability to other experimental situations. When analyzing the reflectance of a dielectric film placed upon a medium whose modulus of the complex index is higher, one runs into many more mathematical and computational difficulties (Ref. 7). The way these problems are attacked is the subject of Section 3.0.

In Section 4.0 the multiple-film thickness method, which is incorporated in the computer program RENLIN, is described.

## 2.0 EXTRACTION OF THE OPTICAL CONSTANTS OF A THIN FILM FROM TRANSMISSION MEASUREMENTS OF A SINGLE-FILM THICKNESS

When determining the complex refractive index $\hat{n} = n + ik$ of thin films, most investigators have used the observed dependence of transmittance upon film thickness. (See, for example, Refs. 1 through 4.) However, Maeda et al. (Ref. 8) have employed a Kramers-Kronig (KK) dispersion relationship which allowed a calculation of the n- and k-values from the transmittance spectrum of a single-film thickness. These authors used measurements of the transmittance relative to that at zero-film thickness. Unfortunately, errors most likely associated with estimates of quantities outside of the wavenumber domain of their data caused very noticeable distortions in their computed n- and k-spectra.

Described in this section is a new subtractive Kramers-Kronig (SKK) algorithm which gives highly reliable n- and k-spectra from measurements of the absolute transmittance of a single, uniform thin film deposited on a uniform thick substrate. Not only can this program reduce the number of necessary experimental measurements, it is also capable of noting any differences in the optical constants of the film material due to changes in film thickness.

### 2.1 THEORY

Several authors (Refs. 1 through 5 and 8 through 10) have discussed the transmittance of a light beam through a thin film on a thick substrate where all surfaces are planar, parallel, and, ideally, infinite in extent (Fig. 1). For normal incidence of a semi-infinite light beam, the absolute transmittance $T(\nu)$ at wavenumber $\nu$ is given by (Refs. 1, 5, and 8)

$$T(\nu) = \hat{t}^*(\nu)\hat{t}(\nu) \tag{1}$$

where t is the complex normal transmission coefficient of the film (medium 1 in Fig. 1) and the substrate (medium 2) bounded by semi-infinite media 0 and 3. The asterisk indicates the complex conjugate of a complex quantity.

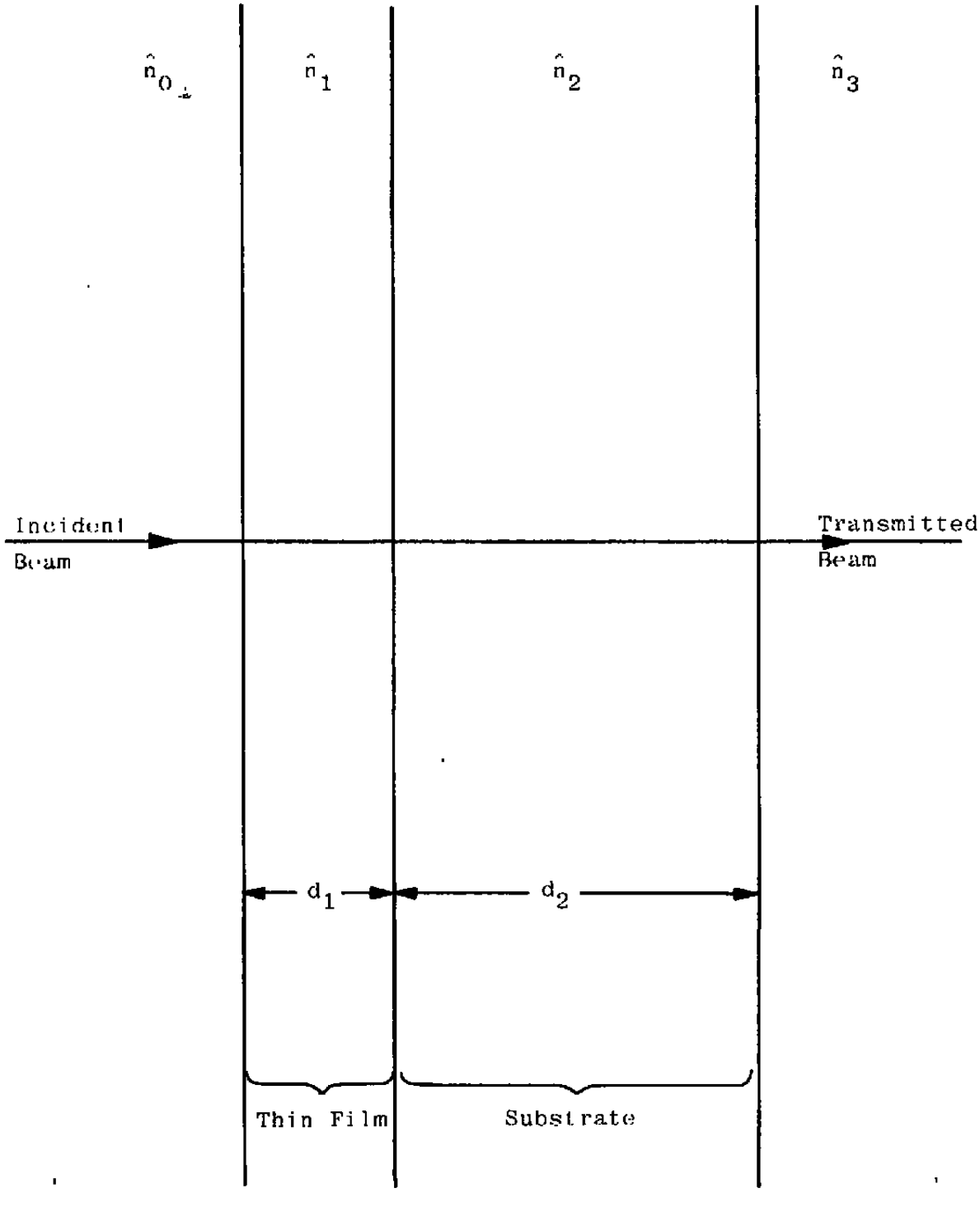


**Figure 1. Geometry depicting analytical model for a thin film formed upon a thick substrate.**

The transmission coefficient is

$$\hat{t} = |\hat{t}_{23}|\,\hat{t}_{012}\exp(-\beta_2 d_2)/[1 - |\hat{r}_{23}|^2\,|\hat{r}_{210}|^2\exp(-4\beta_2 d_2)]^{1/2} \tag{2}$$

where the complex Fresnel transmission coefficient $\hat{t}_{jm}$ and the reflection coefficients $\hat{r}_{jm}$ at the interface of the incident (j) and refracted (m) media are

$$\hat{t}_{jm} = 2\hat{n}_j/(\hat{n}_j + \hat{n}_m) \tag{3}$$

and

$$\hat{r}_{jm} = (\hat{n}_j - \hat{n}_m)/(\hat{n}_j + \hat{n}_m) \tag{4}$$

for normal incidence. In Eq. (2), $\hat{t}_{012}$ represents the complex transmission coefficient for a beam going from medium 0, through the film of thickness $d_1$, and into medium 2, the substrate, whose thickness $d_2$ is much larger than the coherence length of the beam. The complex reflection coefficient $\hat{r}_{210}$ refers to a beam incident upon the film within the substrate. These coefficients may be written as

$$\hat{t}_{012} = \hat{t}_{01}\hat{t}_{12}\exp(i\hat{\gamma}_1 d_1)/[1 + \hat{r}_{01}\hat{r}_{12}\exp(2i\hat{\gamma}_1 d_1)] \tag{5}$$

$$\hat{r}_{210} = [\hat{r}_{21} + \hat{r}_{10}\exp(2i\hat{\gamma}_1 d_1)]/[1 + \hat{r}_{21}\hat{r}_{10}\exp(2i\hat{\gamma}_1 d_1)] \tag{6}$$

with

$$\beta_2 = 2\pi\nu k_2 \tag{7}$$

and

$$\hat{\gamma}_1 = 2\pi\nu\hat{n}_1 \tag{8}$$

Each coefficient accounts for the infinite number of reflections within the film which cause thin film interference effects. The quantity $\beta_2$ arises from the absorption of photons within the substrate, whereas $\hat{\gamma}_1$ describes the phase changes as well as the photon absorption from beams traversing the film. Note that the denominators of $\hat{t}_{012}$ and $\hat{r}_{210}$ are equal because $\hat{r}_{jm} = -\hat{r}_{mj}$ by Eq. (4).

Equations (1) through (8) show the dependence of the transmission coefficient $\hat{t}$, and thus the transmittance T, upon eleven parameters: wavenumber $\nu$, film and substrate thickness $d_1$ and $d_2$, and the real and imaginary parts of $\hat{n}_0$, $\hat{n}_1$, $\hat{n}_2$, and $\hat{n}_3$. One method of finding any unknown parameters is to vary at least one other parameter in a known manner

so that the number of separate measurements of T at a given wavenumber is at least as great as the number of unknown parameters. For example, if only the film optical constants $n_1$ and $k_1$ are unknown, the transmittance T must be measured at least twice at every wavenumber using different known values of the film thickness $d_1$ (Refs. 1 through 4). Because closed-form solutions for $n_1$ and $k_1$ from Eqs. (1) through (8) are not possible, the authors of Ref. 1 utilized the nonlinear least-squares algorithm of Marquardt (Ref. 11) in computer program TRNLIN.

Alternatively, the minimum number of experiments may be reduced to half that required for the previous method if it is possible to measure $t(\nu)$ instead of just $T(\nu)$ at the desired wavenumbers. In this report, values of the optical constants $n_1$ and $k_1$ of the film are unknown and the nine other parameters in Eqs. (1) through (8) are known. By finding t at the wavenumbers of interest, experiments may be done on just one film thickness instead of making observations of at least two different film thicknesses when only T is obtained.

The equation

$$\hat{t}(\nu) = [T(\nu)]^{1/2} \exp[i\phi(\nu)] \tag{9}$$

can be used provided that $\phi(\nu)$, the change in phase of the transmitted light beam relative to that of the incident beam at the 0-1 interface, can be found. [Note that Eq. (2) implies that $\hat{t}$ and $\hat{t}_{012}$ share the same arcus, or phase angle.] Direct measure of $\phi$ is difficult, expecially for transmittance. However, far-infrared asymmetric Fourier-transform spectroscopy can yield phase information for reflected beams (Refs. 12 through 15).

Even if the phase $\phi(\nu)$ cannot be directly observed, it may yet be determined from any one of several equivalent relationships including the widely-used Kramers-Kronig (KK) dispersion relations, the Fourier-allied integrals (Refs. 16 and 17), and the Fourier-conjugate series (Ref. 18). In this work, a modified form of the KK dispersion equations known as the subtractive Kramers-Kronig (SKK) relations (Refs. 1 and 19) is used. Ahrenkiel (Ref. 19) has shown that errors associated with the extrapolations which must be applied to the data because of its finite extent are reduced in the SKK formulation.

### 2.1.1 Determination of Phase $\phi$ of $\hat{t}$

Following Maeda et al. (Ref. 8), the model described in Eqs. (1) through (8) and pictured in Fig. 1, is the KK relation

$$\phi(\nu) + 2j\pi = \frac{2\nu}{\pi} P \int_0^\infty \frac{\ln |\hat{t}(\nu')|\, d\nu'}{\nu'^2 - \nu^2} + 2\pi\nu d_1$$

$$= -\frac{\nu}{\pi} P \int_0^\infty \frac{\ln T(\nu')}{\nu'^2 - \nu^2} d\nu' + 2\pi\nu d_1 \tag{10}$$

where j is an integer and P indicates that the Cauchy principal value of the integral is to be used. The value of the integer j is immaterial if $\hat{t}(\nu)$ is computed by Eq. (9). However, its value is not arbitrary and must be known where the SKK relations are used.

### 2.1.2 Derivation of the SKK Relation

If at $\nu = \nu_0$ the optical constants of the film material under study are obtained from a prior measurement, then measurements of the optical constants at other wavenumbers may be based upon those at $\nu = \nu_0$ in the following manner. At $\nu = \nu_0$, Eq. (10) is

$$\phi(\nu_0) + 2m\pi = -\frac{\nu_0}{\pi} P \int_0^\infty \frac{\ln T(\nu')}{\nu'^2 - \nu_0^2} d\nu' + 2\pi\nu_0 d_1 \tag{11}$$

where the integer m is not necessarily equal to j in Eq. (10). Combining Eqs. (10) and (11) gives

$$\frac{\phi(\nu) + 2j\pi}{\nu} - \frac{\phi(\nu_0) + 2m\pi}{\nu_0} = \frac{\nu_0^2 - \nu^2}{\pi} P \int_0^\infty \frac{\ln T(\nu')}{(\nu'^2 - \nu^2)(\nu'^2 - \nu_0^2)} d\nu'$$

or

$$\phi(\nu) + 2j\pi = \frac{\nu}{\nu_0}[\phi(\nu_0) + 2m\pi] + \frac{\nu(\nu_0^2 - \nu^2)}{\pi} P \int_0^\infty \frac{\ln T(\nu')}{(\nu'^2 - \nu^2)(\nu'^2 - \nu_0^2)} d\nu'$$

To make $\phi(\nu)$ a function of $\nu$ (i.e., a single-valued relation), j must equal m because at $\nu = \nu_0$, the last equation is $\phi(\nu_0) + 2j\pi = \phi(\nu_0) + 2m\pi$. Thus,

$$\phi(\nu) + 2m\pi = \frac{\nu}{\nu_0}[\phi(\nu_0) + 2m\pi] + \frac{\nu(\nu_0^2 - \nu^2)}{\pi} P \int_0^\infty \frac{\ln T(\nu')}{(\nu'^2 - \nu^2)(\nu'^2 - \nu_0^2)} d\nu' \tag{12}$$

Usually the values of n and k of the film at $\nu_0$ are known from previous experiments. Equations (2) through (8) are used to compute $\hat{t}(\nu_0)$ and then find $\phi(\nu_0)$ from

$$\phi(\nu_0) = \tan^{-1}\left\{\mathrm{Im}[t(\nu_0)]/\mathrm{Re}[t(\nu_0)]\right\} \tag{13}$$

where $\tan^{-1}$ (corresponding to subroutine DATAN2 in FORTRAN IV) has a range interval of $(-\pi, \pi)$ and selects the value that lies in the same quadrant in which $\hat{t}(\nu_0)$ lies when drawn in the complex plane.

### 2.1.3 Determination of the Integer m in Eq. (12)

In order to use the SKK relationship in Eq. (12), the integer m must be evaluated, which by Eq. (11) is

$$m = -\frac{\nu_0}{2\pi^2} P \int_0^\infty \frac{\ln T(\nu')}{\nu'^2 - \nu_0^2} d\nu' - \frac{\phi(\nu_0)}{2\pi} + \nu_0 d_1 \tag{14}$$

While the numerical evaluation of the integral in Eq. (14) is straightforward, it is nonetheless tedious and lengthy because of the difficulties involved with calculating the contributions to the integral from the wavenumber domain near the singular point $\nu' = \nu_0$. Fortunately, the integral term is almost always much smaller than the algebraic sum of the other two terms in Eq. (14) and may be safely approximated by the integral term.

Let

$$\ln T(\nu) \approx \ln T_0 - \sum_{j=1}^{N} a_j\, \delta(\nu - \nu_j)$$

in which $T_0$ represents an average value of the absolute transmittance over those wavenumber regions far away from an absorption band, N is the number of significant absorption bands, $\nu_j$ is the wavenumber at the minimum transmittance of the $j^{th}$ band, and $\delta$ is the Dirac delta "function." The constants $a_j$ are $a_j = \ln |T_0/T(\nu_j)|$, so now

$$\ln T(\nu) \approx \ln T_0 + \sum_{j=1}^{N} \ln [T(\nu_j)/T_0]\, \delta(\nu - \nu_j) \tag{15}$$

The integral of Eq. (14) becomes

$$P \int_0^\infty \frac{\ln T(\nu')}{\nu'^2 - \nu_0^2} d\nu' \approx P \int_0^\infty \frac{\ln T_0}{\nu'^2 - \nu_0^2} d\nu' + P \int_0^\infty \sum_{j=1}^{N} \frac{\ln[T(\nu_j)/T_0]\delta(\nu' - \nu_j)}{\nu'^2 - \nu_0^2} d\nu'$$

The first integral on the right-hand side is zero because $\ln T_0$ is constant, and

$$P \int_0^\infty \frac{d\nu'}{\nu'^2 - \nu_0^2}$$

is zero. The second integral becomes

$$\sum_{j=1}^{N} \frac{\ln[T(\nu_j)/T_0]}{\nu_j^2 - \nu_0^2}$$

giving as an approximation to Eq. 14,

$$m \approx \frac{\nu_0}{2\pi^2} \sum_{j=1}^{N} \frac{\ln[T_0/T(\nu_j)]}{\nu_j^2 - \nu_0^2} - \frac{\phi(\nu_0)}{2\pi} + \nu_0 d_1 \tag{16}$$

In the present study, $T_0$ is chosen to be $T(\nu_0)$.

### 2.1.4 Estimation of the Complex Index of Refraction $\hat{n}$ of the Film

Many times in the course of extracting the complex index of refraction $\hat{n}(\nu) = n(\nu) + ik(\nu)$ of the film from the value of the complex transmission coefficient $\hat{t}(\nu)$, it is found that several different pairs of n- and k-values will yield identical $\hat{t}(\nu)$ values when each pair is substituted, in turn, into Eqs. (2) through (8). In order to select the "best" pair of values on physical grounds, it is necessary to resort to a cruder model of the experimental setup from which approximate values n and k are obtained.

Near strong film absorptions, beams traversing the film are rapidly attenuated. As a consequence, nearly all of the photons which have frequencies that are readily absorbed by the film, but nonetheless appear in the transmitted beam, have passed through the film just once. If all of the photons in the transmitted beam have traversed the film only once, and if $I_3/I_0$ is the observed ratio of the transmitted beam intensity $I_3$ to the incident beam intensity $I_0$, an estimate of k is (Ref. 1)

$$k \approx \ln\left[|\hat{n}_3/\hat{n}_0|\, T_s/(I_3/I_0)\right]/(4\pi\nu d_1) \tag{17}$$

where the transmittance $T_s$ of the bare substrate is

$$T_s = \hat{t}^*_s \hat{t}_s \tag{18}$$

and

$$\hat{t}_s = |\hat{t}_{23}|\,\hat{t}_{02} \exp(-\beta_2 d_2)/[1 - |\hat{r}_{23}|^2 |\hat{r}_{20}|^2 \exp(-4\beta_2 d_2)]^{1/2} \tag{19}$$

[Eq. (19) can be heuristically obtained from Eq. (2) by elimination of the "1" subscript denoting the film.] Often one can put measured values of $T_s$ into the relation indicated in Eq. (17).

Estimates of n are based on an assumed film absorption bandshape as a Cauchy (Lorentzian), Gaussian, Voight, or similar profile. Peiponen (Ref. 20) has derived an expression for n because of an absorption band having the Cauchy form

$$k(\nu) = k_{max}/[1 + (4/\gamma^2)(\nu - \nu_1)^2] \tag{20}$$

Here, $k_{max}$ is the value of k at $\nu = \nu_1$, where $\nu_1$ is the wavenumber at the maximum absorption and $\gamma$ is the difference between the wavenumbers at the half-maximum points, i.e., $\gamma$ is the full-width-at-half-maximum intensity (Fig. 2).

If all N-bands in a spectrum are assumed to have the Cauchy shape of Eq. (20), an approximate expression for n is

$$n(\nu) \approx n_0 + \sum_{j=1}^{N} \frac{k_{maxj}\, \nu \nu_{Lj} (\nu - \nu_j)(\nu_{Lj} - \nu_j)}{\nu_{Lj}^2(\nu - \nu_j)^2 + \nu^2(\nu_{Lj} - \nu_j)^2} \tag{21}$$

Here, $n_0$ is the contribution to n because of absorption outside the wavenumber domain of the data. For the $j^{th}$ band, $\nu_j$ is the wavenumber at which the maximum absorption, $k_{max\,j}$, occurs, and

$$\nu_{Lj} = \nu_j - \gamma_j/2 \tag{22}$$

is the smaller half-maximum intensity wavenumber, where $\gamma_j$ is the difference between the larger half-maximum intensity wavenumber and $\nu_{Lj}$. In this study, $n_0$ was equated with $n(\nu_0)$, and the other parameters were estimated in Eq. (21) from the approximate k-spectrum created by the application of Eq. (17) to all measured $T(\nu)$ values.

### 2.1.5 Extrapolations of the Data

A major problem in using the SKK relation for $\phi(\nu)$ in Eq. (12) is that the integral over the wavenumber in Eq. (12) has the limits zero and infinity. It is necessary to extrapolate the data to these end points, and one now investigates the asymptotic behavior of $\ln T(\nu)$ for the two limits $\nu \to \infty$ and $\nu \to 0$.

As $\nu$ approaches infinity, the electrons in any material become more nearly "free," and the dielectric constant may be written (Refs. 21 and 22) as $\hat{\epsilon}(\nu) = \hat{n}^2(\nu) \approx 1 - \nu_p^2/\nu^2$, which means

$$\hat{n}(\nu) \approx -\nu_p^2/(2\nu^2) \tag{23}$$

where

$$\nu_p = \omega_p/(2\pi c) = 2\eta e^2/(m_e c) \tag{24}$$

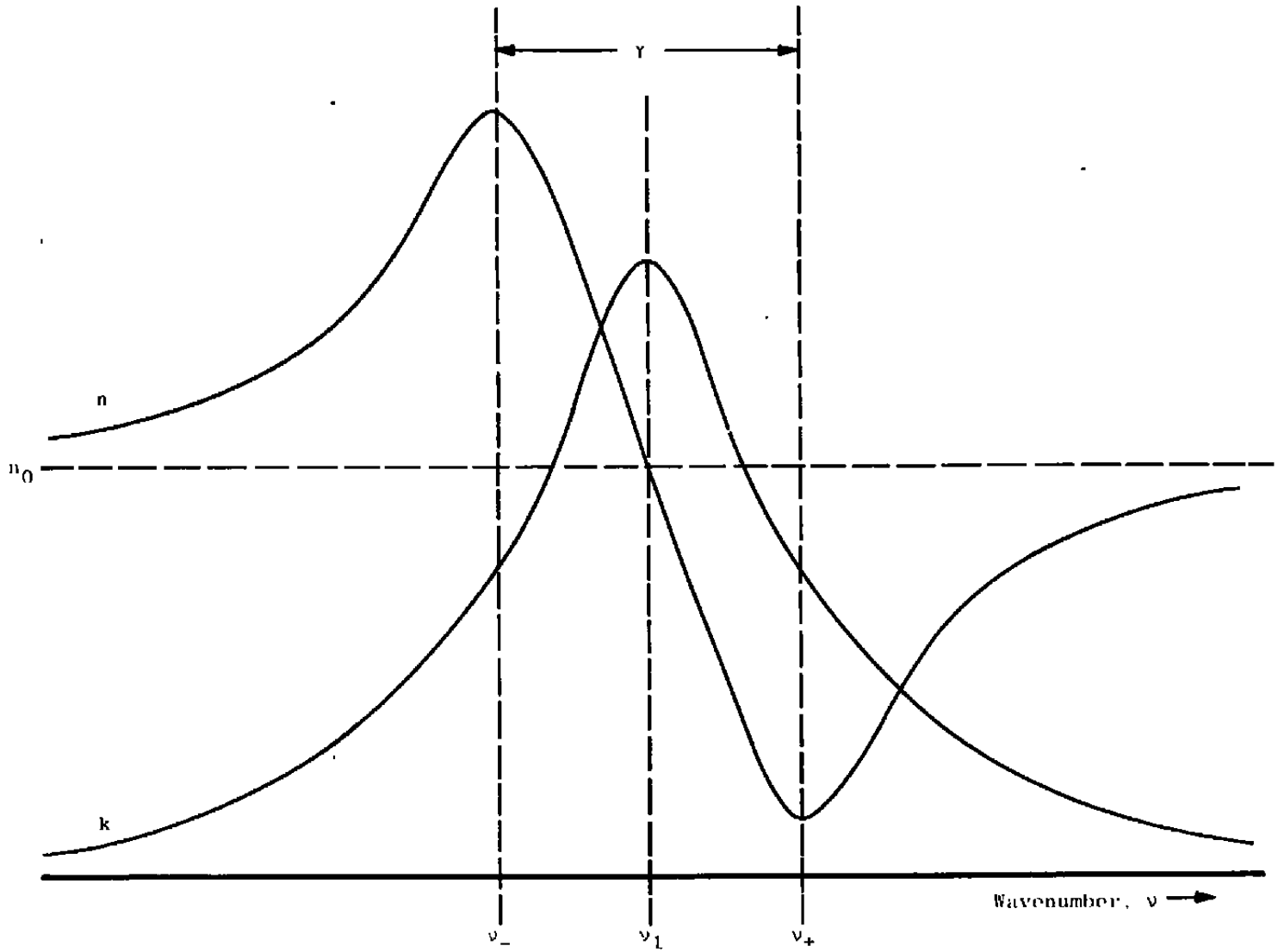


**Figure 2. Refractive and absorption indices of an absorption having a Cauchy (Lorentzian) bandshape.**

$\omega_p$ is the "plasma frequency", $\eta$ is the number density of free electrons, $m_e$ is the mass of a free electron, e is the electronic charge, and c is the speed of light in vacua. It follows from the relations given in Eqs. (1) through (8) that as $\nu$ approaches infinity,

$$\hat{t}_{jm}(\nu) \approx 1 + (\nu_{pm}^2 - \nu_{pj}^2)/(4\nu^2)$$

$$\hat{r}_{jm}(\nu) \approx (\nu_{pm}^2 - \nu_{pj}^2)/(4\nu^2) = \hat{t}_{jm}(\nu) - 1$$

yielding

$$|\hat{t}_{012}|^2 = \hat{t}_{012}^* \hat{t}_{012} \approx [1 + \nu_{p2}^2/(4\nu^2) + \ldots]^2$$

$$|\hat{r}_{210}|^2 = \hat{r}_{210}^* \hat{r}_{210} \approx [2\nu_{p1}^2(\nu_{p1}^2 - \nu_{p2}^2) + \nu_{p2}^4 + \ldots]/(16\nu^4)$$

and, finally,

$$T = \hat{t}^* \hat{t} \approx 1 - \nu_{p2}^2/(8\nu^4) + \ldots \text{ or, } \ln T \approx -\nu_{p2}^4/(8\nu^4) \tag{25}$$

Here, $\nu_{pj}$ is the critical "plasma wavenumber" defined in Eq. (24) for the $j^{th}$ medium, and $\nu_{p0} = \nu_{p3} = 0$ because in this experiment these media are essentially vacuums.

As $\nu$ approaches zero, for dielectrics (Refs. 21 and 22),

$$\hat{\epsilon}(\nu) = \hat{n}^2(\nu) \approx \epsilon_0 \tag{26}$$

a constant, whereas for conductors

$$\hat{\epsilon}(\nu) = \hat{n}^2(\nu) \approx \frac{2i\sigma}{c\nu} \tag{27}$$

where $\sigma$ is the conductivity for constant currents. For the dielectric media of Fig. 1 from Eq. (26),

$$\ln T(\nu) \approx \ln T_0 \tag{28}$$

becomes a constant, as $\nu$ approaches zero.

Equations (25) and (28) are used to calculate the end contribution, A and B, of the integral in Eq. (12). If $\nu_\ell$ is the smallest wavenumber in the data domain, and assuming

$$\ln T(\nu) \approx \ln T(\nu_\ell) \tag{29}$$

the contribution A to the integral over the interval $(0, \nu_\ell)$ is given as

$$A = \frac{\nu(\nu_0^2 - \nu^2)}{\pi} P \int_0^{\nu_\ell} \frac{\ln T(\nu')}{(\nu'^2 - \nu_0^2)(\nu'^2 - \nu^2)} d\nu'$$

$$\approx \frac{\nu}{2\pi}\left(\frac{1}{\nu} \ln\left|\frac{\nu_\ell + \nu}{\nu_\ell - \nu}\right| - \frac{1}{\nu_0} \ln\left|\frac{\nu_\ell + \nu_0}{\nu_\ell - \nu_0}\right|\right) \tag{30}$$

Likewise if $\nu_u$ is the greatest wavenumber in the data domain, assume, following Eq. (25),

$$\ln T(\nu) \approx (\nu_u^4/\nu^4) \ln T(\nu_u) \tag{31}$$

in the interval $(\nu_u, \infty)$. The end contribution B over $(\nu_u, \infty)$ is

$$B = \frac{\nu(\nu_0^2 - \nu^2)}{\pi} P \int_{\nu_u}^{\infty} \frac{\ln T(\nu')}{(\nu'^2 - \nu_0^2)(\nu'^2 - \nu^2)} d\nu' \approx \frac{\nu(\nu_0^2 - \nu^2)\, \nu_u^4 \ln T(\nu_u)}{\pi}$$

$$\left[\frac{\nu_0^2 + \nu^2}{\nu_u\, \nu_0^4\, \nu^4} + \frac{1}{3\, \nu_u^3\, \nu_0^2\, \nu^2} + \frac{1}{\nu_0^4(\nu_0^2 - \nu^2)}\left(\frac{1}{2\nu_0} \ln\left|\frac{\nu_u + \nu_0}{\nu_u - \nu_0}\right|\right)\right.$$

$$\left. + \frac{1}{\nu^4(\nu_0^2 - \nu^2)}\left(\frac{1}{2\nu} \ln\left|\frac{\nu_u + \nu}{\nu_u - \nu}\right|\right)\right] \tag{32}$$

## 2.2 COMPUTER PROGRAM SKKTRANS

The FORTRAN IV computer program called SKKTRANS extracts the optical parameters $n(\nu)$ and $k(\nu)$ of a film material from the absolute transmittance data of a single fixed film and substrate surrounded by a vacuum. The experimental geometry was assumed to be that of Fig. 1 with the physical description contained in Eqs. (1) through (8). It was further assumed that the user would supply a pair of n- and k-values which had been obtained in a separate experiment at $\nu = \nu_0$, a wavenumber that is not at, or next to, the ends of the wavenumber domain of the data. In this program, then, $\hat{n}_0 = \hat{n}_3 = 1$ by assumption, and the user must enter the rest of the parameters: film and substrate thicknesses $d_1$ and $d_2$ and the refractive index $n_2$ of the substrate.

The program SKKTRANS is divided into three main segments, "MAIN," "KAMKON," and "NLNSYS." In MAIN, the computer reads the title card, job parameters, and the data, which are either on cards or in temporary direct-access storage if the data were originally on tape. (The program reads tape data and places it into storage in the jobsteps prior to MAIN.) The data need not be equally spaced in wavenumber.

The second and third parts of SKKTRANS calculate the optical constants of the film, one wavenumber at a time. KAMKON calculates $\hat{t}(\nu)$ and passes it on to NLNSYS which finds $n(\nu)$ and $k(\nu)$.

### 2.2.1 Program Segment KAMKON

In KAMKON, the computer recovers the necessary phase information by computing the change of phase $\phi(\nu)$ of the transmitted beam using the SKK relation [Eq. (12)] and the integer value for m that is closest to the right-hand side of Eq. (16). The computer then finds the value of the complex transmission coefficient $\hat{t}(\nu)$ using Eq. (9).

The computer algorithm in KAMKON which evaluates the SKK integral of Eq. (12) is very similar to algorithms in other SKK programs which previously were supplied to AEDC (Ref. 1). KAMKON performs the integration by using Simpson's rule except near the singular points $\nu' = \nu_0$ and $\nu' = \nu$, or whenever the wavenumber separations between three successive data points are unequal. In these exceptional cases, the numerator of the integrand, $\ln T(\nu)$, is approximated by a quadratic function of $\nu$ fitted to the data point at the wavenumber of interest and the two surrounding data points. The computer uses an analytical expression to evaluate the contribution to the integral for these three data points and computes the end corrections from Eqs. (30) and (32).

### 2.2.2 Program Segment NLNSYS

NLNSYS uses the value of $\hat{t}(\nu)$ that is found in KAMKON and calculates the film optical constants $n(\nu)$ and $k(\nu)$. It is not possible to solve for the complex refractive index $n_1$ in Eqs. (2) through (8), and, consequently, NLNSYS incorporates a nonlinear iterative interpolation scheme very similar to Marquardt's nonlinear least-squares algorithm (Ref. 11). However, the converged values of the optical constants which the present algorithm provides cannot meet the least-squares criterion because the algorithm employs two known quantities, the real and imaginary parts of $\hat{t}(\nu)$, to find two unknown quantities, $n(\nu)$ and $k(\nu)$.

#### 2.2.2.1 Selection of the "Best" Pair of Optical Constants

Always from strong absorptions, the algorithm in NLNSYS almost always converges to the "best" pair of n- and k-values, when the initial guesses of these values are the

corresponding "best" values from the calculation just prior to the present one. In spectral regions far from strong absorptions, the "best" pair of values is the pair in which n is not too far from unity and k is close to zero. The other pairs of n- and k-values which satisfy Eqs. (2) through (8) are usually not close to the "best" pair of values.

If the absorption is strong at the wavenumber of interest, however, one may not be able to readily distinguish the "best" pair of n- and k-values from the other possibilities. In this case, NLNSYS uses at least eleven different initial guesses for n and k, and usually finds more than one distinct pair of converged n- and k-values. NLNSYS uses the approximate values of n and k, given in Eqs. (21) and (17), respectively, to help in the selection of the "best" pair.

Theoretically, if the absorption band has the Cauchy, or Lorentzian, shape of Eq. (20), the n-values reach a maximum very near the wavenumber $\nu-$ at the lower half-maximum point, and a minimum very near the wavenumber $\nu+$ corresponding to the upper half-maximum intensity point (Refs. 20 and 23). Thus, in the wavenumber interval $(\nu-, \nu+)$ n should increase monotonically with increasing $\nu$ and vice versa (Fig. 2).

Experimentally, measurement errors, non-Cauchy bandshapes, and the use of approximate n- and k-values often cause shifts in the location of the extremal values of n. Therefore, expect to find the experimental maximum n-value within the interval $(\nu_- - \delta, \nu_- + \delta)$ and the minimum within the interval $(\nu_+ - \delta, \nu_+ + \delta)$, where $\delta$ is typically 3 $cm^{-1}$ or so. Within the two intervals, the n-values should not be rapidly changing, and NLNSYS chooses as "best" the pair of n- and k-values closest (in the n, k-plane) to the n- and k-values found in the last calculation.

Outside of the two wavenumber intervals mentioned above, NLNSYS usually picks as the "best" values the pair closest to the approximate n- and k-values for that wavenumber. The only exceptions occur when the wavenumber of the calculation is within the interval $(\nu_- + \delta, \nu_+ - \delta)$, and the n-value chosen as "best" by the above criteria is less than 0.9 of the n-value found at the larger wavenumber of the last calculation. (In SKKTRANS, the calculations proceed in descending wavenumber.) Because in this interval the n-values should increase monotonically with decreasing wavenumber, NLNSYS chooses as "best" the pair having the smallest n-value that equals or exceeds 0.9 of the best n-value from the previous calculation.

## 2.3 PRELIMINARY RESULTS FROM SKKTRANS

At the time of this writing, some minor debugging of SKKTRANS may still be necessary. However, tests have been made on the reliability of the SKK and interpolation algorithms

using a theoretical transmittance spectrum. The effects of varying the film thickness, using some existing AEDC cryofilm data, also have been noted.

### 2.3.1 Test of the SKK and the Interpolation Algorithms

A theoretical $CO_2$ cryofilm transmittance spectrum was used to test the algorithms in SKKTRANS. This transmittance spectrum, extending from 700 to 3700 $cm^{-1}$, was computed by substituting the n- and k-values of pure solid $CO_2$ cryofilms at 20 K (Ref. 24) into Eqs. (1) through (8). This spectrum was then processed by SKKTRANS in an effort to recover the original n- and k-values.

Note that the SKKTRANS did not simply reverse the calculation process involved in computing the test transmittance spectrum. This can be done only when t is known instead of T. SKKTRANS does compute $\hat{t}$, by first finding $\phi$, and then it calculates the optical constants in an iterative scheme that is essentially a trial-and-error method. Also note that the computation of n and k at a single wavenumber requires the transmittance values at all wavenumbers included in the data because of the SKK relation for $\phi$ [Eq. (12)].

In essence, the validity of the numerical approximation of the SKK relations [Eqs. (12), (13), (30), and (32)] was tested. Figure 3 shows the excellent agreement of the SKKTRANS n-values with the original n-values even near the intense $\nu_3$ band of $12_{CO_2}$. Here, the complex refractive index of the film is the least-squares value $\hat{n} = 1.2220 + i0$ at the wavenumber $\nu_0 = 2700\ cm^{-1}$, and the $CO_2$ film thickness is taken as 2.071 $\mu$m. The data points included in the SKK algorithm extend from 710 to 3690 $cm^{-1}$ and are spaced every 10 $cm^{-1}$, except near significant absorptions. For this film and all others discussed in this report, the substrate is 20 K germanium 4 mm in thickness with a complex index of refraction $n_2 = n_g + i0$ where, correcting Eq. (14) of Ref. 1,

$$n_g(\nu) = A + BL + CL^2 + D\nu^{-2} + E\nu^{-4}$$

$$A = 3.880$$

$$B = 3.91707 \times 10^{-9}\ cm^2$$

$$C = 1.63492 \times 10^{-17}\ cm^4$$

$$D = -600\ cm^2$$

$$E = 5.3 \times 10^8\ cm^4$$

and

$$L = (\nu^{-2} - 2.8 \times 10^{-8}\ cm^2)^{-1} \tag{33}$$

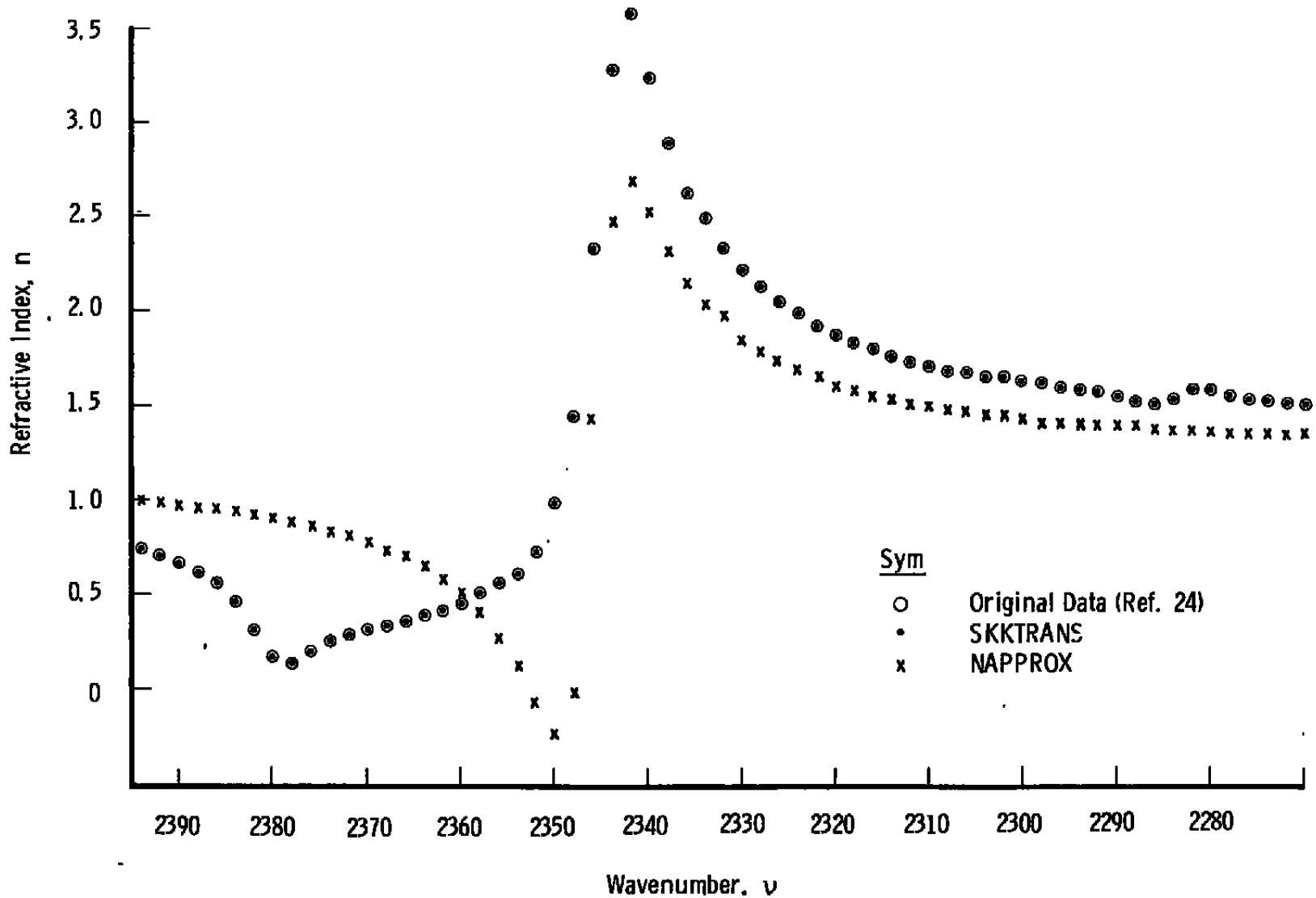


**Figure 3. Refractive index of solid $CO_2$ on 20-K germanium.**

Differences between the SKKTRANS n-spectrum and the original are discernible only near the relative extrema of the n-spectra. The exceptionally close agreement of the SKKTRANS k-spectrum with the original is evident in Fig. 4, and it was concluded that the SKK model and the approximations can faithfully reproduce the original spectra.

Figure 3 also includes a plot of the approximate n-spectrum (NAPPROX) computed from Eq. (21). These approximate values vary widely from the other two spectra because the $\nu_3$ band of $12_{CO_2}$ is highly asymmetric and does not fit the single Cauchy (Lorentzian) bandshape assumed in the calculation of the approximate n-spectrum. Nevertheless, the criteria discussed in Section 2.2.2.1 for choosing the "best" n- and k-values work well even in this case of a poor approximation of the n-spectrum.

On the other hand, observe in Fig. 4 the good agreement of the approximate k-values, from Eq. (17), with the other k-spectra. As expected from the assumptions in the derivation of Eq. (17), this agreement is relatively closer as the k-values increase. The results are in contrast to the conclusion of Maeda et al. (Ref. 8), that the approximate, or "experimental", k-values of Eq. (17) are highly distorted from the "true" KK or SKK values contained in Eqs. (10) and (12).

### 2.3.2 Variation of $\phi(\nu_o) + 2m\pi$ with Film Thickness

When Eq. (16) was derived, it was assumed the Cauchy principal value term in Eq. (11) was small enough to make $\phi(\nu_0) + 2\ m\pi$ nearly linearly dependent upon the film thickness $d_1$. [$\phi(\nu_0) + 2\ m\pi$ is the phase change of the radiation in the transmitted beam having wavenumber $\nu_0$.] SKKTRANS determines $\phi(\nu_0)$ from Eq. (13) and uses Eq. (16) to find m. Thus, a plot of the SKKTRANS values of $\phi(\nu_0) + 2\ m\pi$ versus film thickness is an independent check of Eq. (11) and the assumption of linearity.

In Fig. 5 are seen the $\phi(\nu_0) + 2\ m\pi$ values found by SKKTRANS for 15 different thicknesses, ranging from 0.2633 to 4.476 $\mu$m, of films formed when a gaseous mixture of $N_2$ (74.7 mole percent) and $CO_2$ (25.3 mole percent) impinges on a 20-K germanium substrate (Ref. 1). To a good approximation the plot is linear and passes through the origin, and the regression line (dashed line) through the data has a slope of 1.69967 $\mu m^{-1}$. In Eq. (11), the value of $2\ \pi\nu_0(\nu_0 = 2144\ cm^{-1})$ is 1.34711 $\mu m^{-1}$ which has a relative difference of 20.7 percent with the experimental slope. Because the authors of Ref. 1 found the film thicknesses from the interference pattern of He-Ne laser beams reflected from the film, it is possible that a systematic error entered the thickness measurements. In this instance, increasing each of the measured thickness values by a factor of 1.69967 $\mu m^{-1}$/1.34711 $\mu m^{-1}$ = 1.26171 would cause the experimental slope to be identical with the theoretical slope, $2\ \pi\nu_0$. However, other tests (Section 2.3.3) do not support the above changes in the

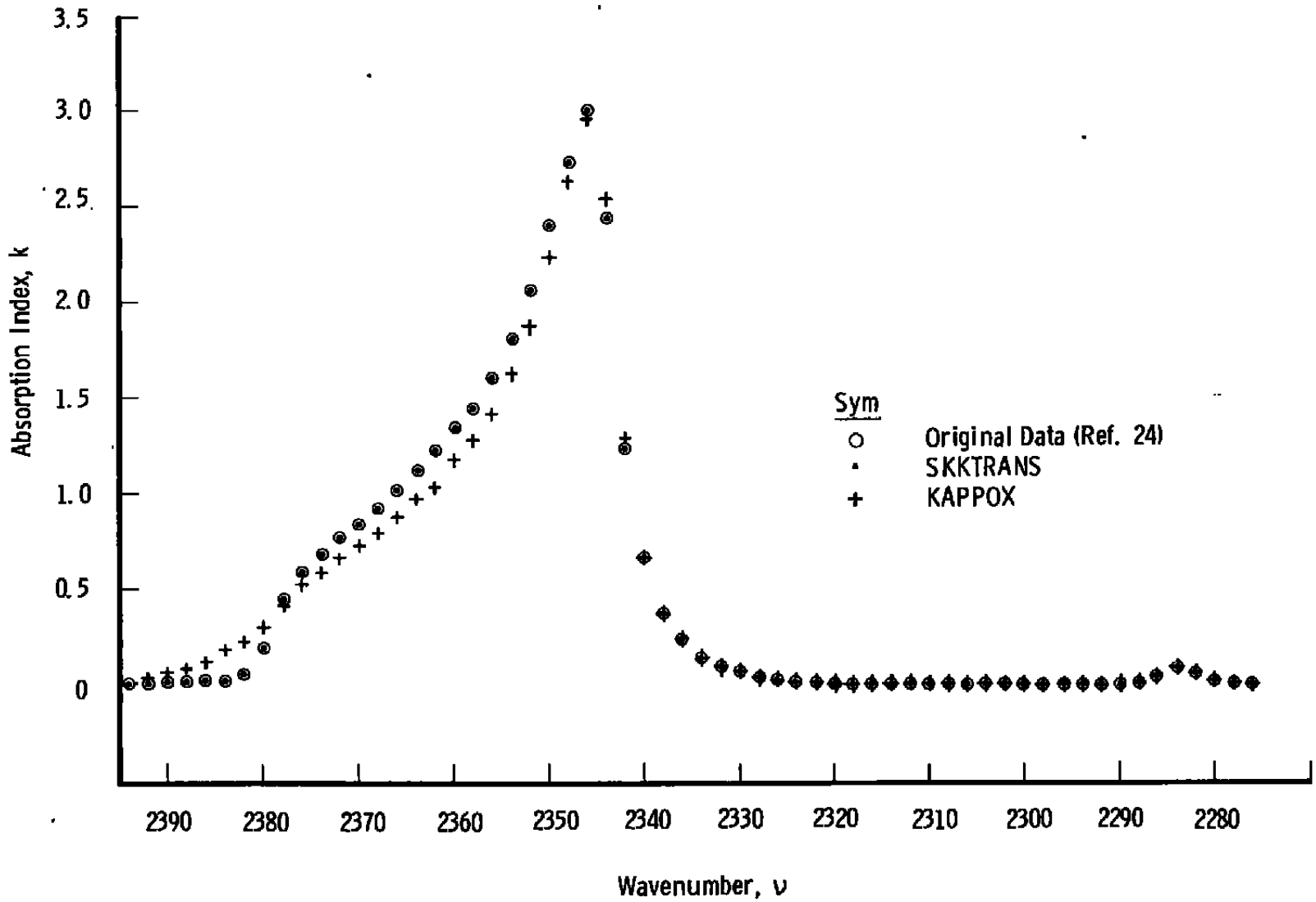


**Figure 4. Absorption index of solid $CO_2$ on 20-K germanium.**

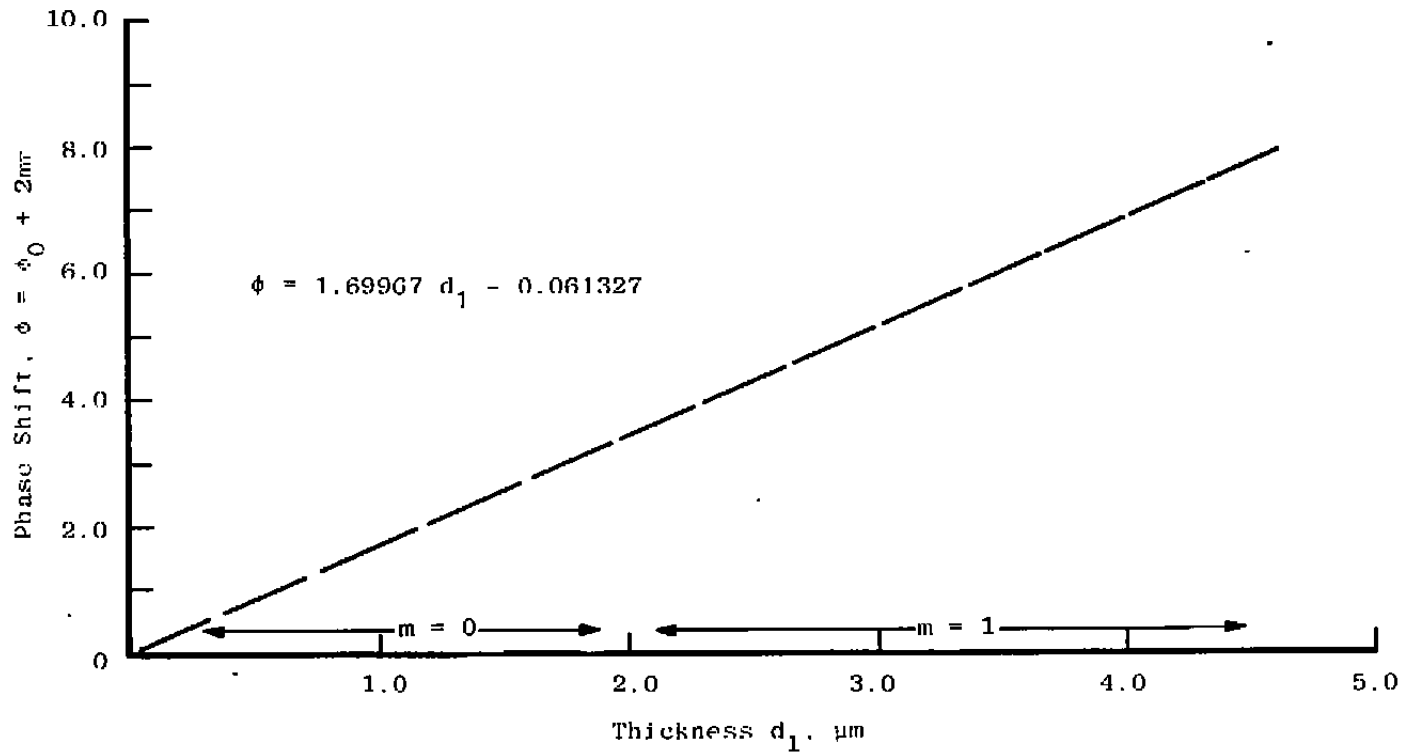


**Figure 5. Plot of phase shift $\phi = \phi_0 + 2m\pi$ at $\nu_0 = 2144\ cm^{-1}$ of $N_2/CO_2$ (74.7%/25.3%) films at 20-K germanium.**

thicknesses, nor does the experimental error estimated by the authors of Ref. 1 allow so great a discrepancy. At any rate, it appears, at least for $N_2/CO_2$ films, that $2\pi\nu_0 d_1$ is the dominant term of Eq. (11).

### 2.3.3 Changes in the n- and k-Spectra as a Function of Film Thickness $d_1$

As the thickness of a film changes, the transmittance spectrum changes in appearance. However, if it is assumed that the films are uniform and homogeneous in composition regardless of thickness, two films of the same material, but having different thicknesses, should yield the same n- and k-spectra. This assumption is the basis of the least-squares method of analyzing transmittance with thickness to yield the film optical constants. However, the assumption is not true for very thin metal films (Ref. 5). Program SKKTRANS allows one to examine each film thickness separately.

Figures 6 and 7 present the optical constants of the $N_2/CO_2$ films discussed in Section 2.3.2. For each thickness, the data points were spaced 2 $cm^{-1}$ apart and extended from 602 to 3750 $cm^{-1}$. The $n(\nu_0)$- and $k(\nu_0)$-values required in the SKK algorithm were 1.2610 and zero, respectively, and were measured at $\nu_0 = 2144\ cm^{-1}$.

The dashed line in Fig. 7 represents the values of k found in Ref. 1 by a least-squares fit of transmittance to thickness. The authors of Ref. 1 computed values of n by an SKK analysis of the least-squares k-values, and the dashed line in Fig. 6 indicates these n-values. These n- and k-spectra are nearly identical to those of the smallest thickness (0.2633 $\mu$m) even though the least-squares analysis used the transmittance data of 15 different film thicknesses ranging from 0.2633 to 4.4761 $\mu$m. This is because the transmittance at a given wavenumber decreases approximately exponentially with increasing film thickness, and the least-squares criterion is biased in favor of the larger measurements. For the $N_2/CO_2$ films, for example, the measured absolute transmittance at 2350 $cm^{-1}$ was approximately 0.3 for a film 0.2633-$\mu$m thick, whereas the 1.3165-$\mu$m film had a value of about 0.01. If the least-squares procedure had achieved nearly the same absolute error (e.g., 0.01) between the computed and measured transmittance values of these films, the relative error would be about 30 times greater for the thicker film. This means that one can disregard transmittance measurements that are near zero when employing the least-squares method.

There are also reasons to discount nearly-zero transmittance measurements when one makes a KK or SKK analysis. In Figs. 6 and 7 only the SKKTRANS n- and k-spectra of the smallest five thicknesses are shown because the peak absorptions in the ten larger thicknesses are so intense that, because of instrumental drift, the Fourier-transform spectrometer measured the smallest absolute transmittance to be very slightly negative. In cases of this type, a new "baseline" for the transmittance spectrum can be established by adding a very

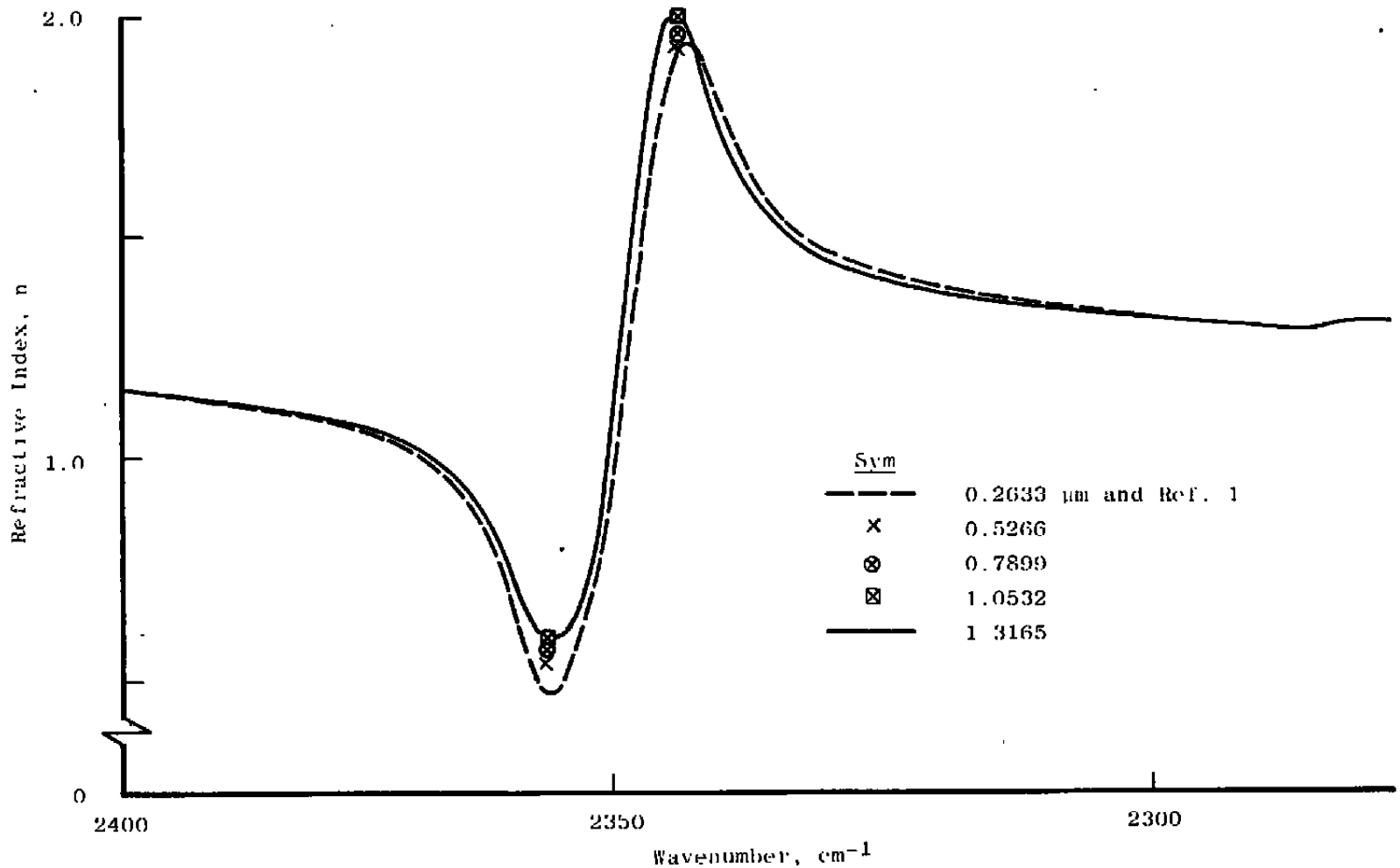


**Figure 6. Refractive index of solid $N_2/CO_2$ mixture (74.7%/25.3%) on 20-K germanium computed at several thicknesses.**

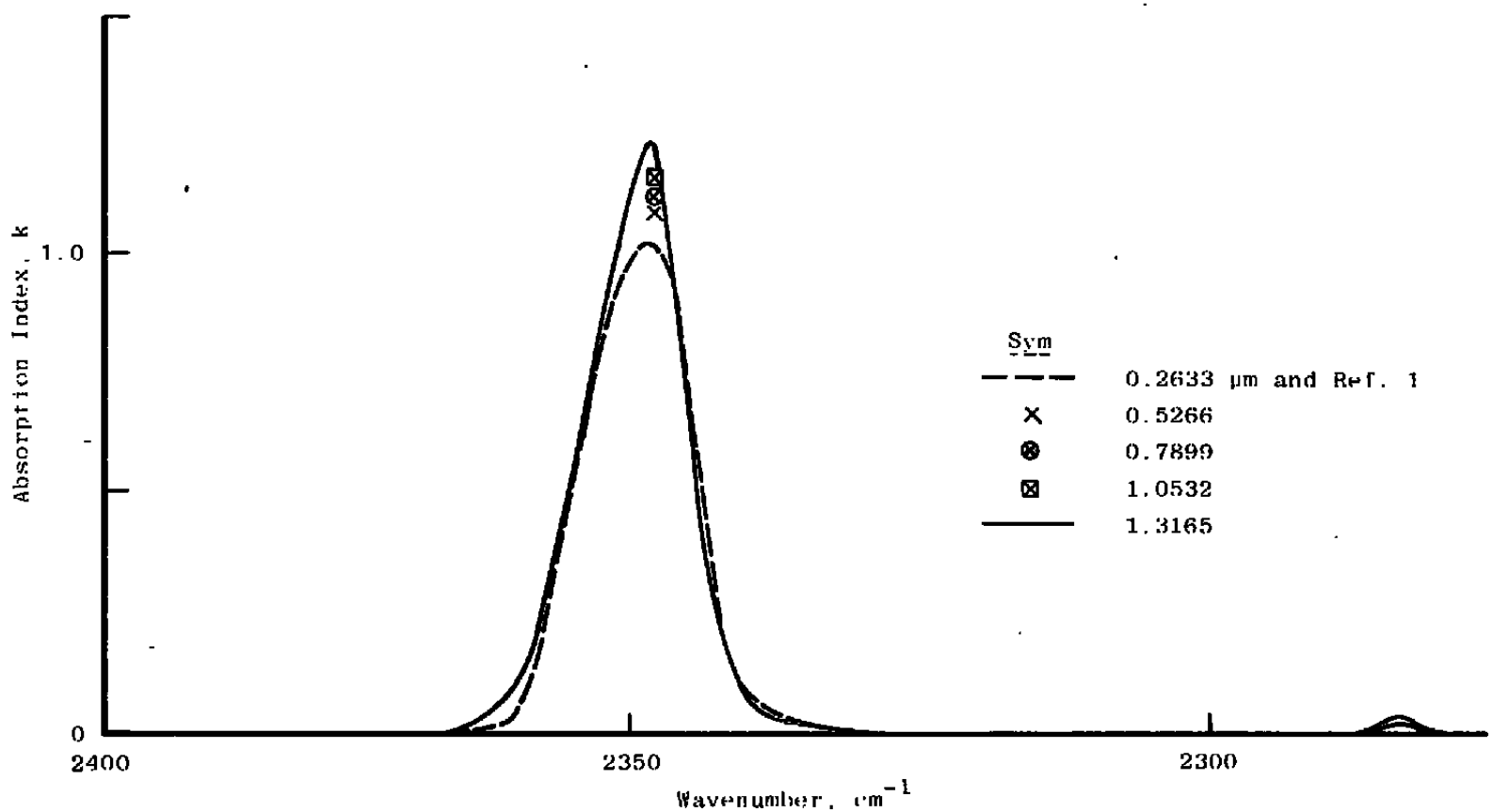


**Figure 7. Absorption index of solid $N_2/CO_2$ mixture (74.7%/25.3%) on 20-K germanium computed at several thicknesses.**

small constant to every original transmittance value so that the new transmittance spectrum will not have any negative (or zero) values.

It is not clear, though, what the additive constant should be. The establishment of the criteria for choosing the constant is very important because relatively small adjustments of the additive constant can cause variances in the smallest transmittances of several hundred percent, or more, and can create very noticeable differences in the n-spectra computed by SKKTRANS. Perhaps it is possible to find a suitable additive constant from "sum rules" akin to those developed by Smith and Manogue (Ref. 25) for reflection spectroscopy.

Note in Figs. 6 and 7 that both the n- and the k-spectra of $N_2/CO_2$ vary slightly and in a nonrandom manner with film thickness. The same effect occurs even more dramatically in thin films of 85% $N_2$/15% $NH_3$, 91% CO/9%$H_2O$, and 93% Ar/7% $H_2O$ condensed onto a 20-K germanium substrate (Ref. 1). Only further investigation can uncover whether this trend is a real physical effect of these films, or a computational artifact due to a systematic error in, e.g., the determination of the film thickness, or inadequacies in the model. As a test of the effects of a systematic error in film thickness, the optical constants of the $N_2/CO_2$ films were recomputed using the SKKTRANS thickness values which were 1.26171 times those given in Figs. 6 and 7. (In Section 2.3.2, it was found that 1.26171 was the ratio of the observed-to-theoretical slopes of the plot in Fig. 5.) Even though the new spectra were not identical to the original, the new spectra showed, to the same degree, the original variance in value with film thickness. At least in this instance, the variation of n and k does not seem to depend on film thickness errors. These examples illustrate the usefulness of obtaining the optical constants of individual films, especially for films such as those containing hydrogen-bonded molecules whose optical properties may depend on film thickness.

## 2.4 USING PROGRAM SKKTRANS

SKKTRANS can be used to extract the optical constants of a uniform thin film from absolute transmittance measurements of the film on a thick substrate surrounded by a vacuum. Experimentally, an absolute transmittance measurement is the ratio of the transmitted beam intensity, at a given wavenumber, to that of the incident beam.

### 2.4.1 Program Parameters

The present version of SKKTRANS calculates the refractive index of the 20-K germanium substrate, $n_2 = n_g$, from Eq. (33). One must enter into SKKTRANS the film and substrate thicknesses and the optical constants of the film at $\nu = \nu_0$, a wavenumber that is not at one of the endpoints of the transmittance data.

The program also requires one to supply the wavenumbers within the data domain at which to start and stop the calculations and to specify how many of the data points used in the SKK algorithm are to be skipped between successive determinations of the film optical constants. The initial guesses of n and k for the first calculation and the maximum number of iterations in the interpolation procedure must also be given.

If the data are on a tape or disk, SKKTRANS constructs a new data set from the original data. The smallest and largest wavenumber must be entered in the new data set and the number of original data points on the tape or disk that are to be skipped when the program picks out the data points to be included in the new set of data. Additional program parameters enable SKKTRANS to write the computed n- and k-values onto a tape. Please note that appropriate changes in the job control language (JCL) must be made for use of tape or disk volumes.

The remaining input parameters have the information needed to find, in the approximate k-spectrum generated by Eq. (17), the wavenumbers at the peak and the two half-intensity points for each major film absorption band. At a wavenumber near a large absorption, SKKTRANS makes multiple optical constant computations and, subsequently, picks the "best" values in the manner described in Section 2.2.2.1. Empirically it was found that absorptions whose peak k-values are a few tenths or less can be ignored.

### 2.4.2 Spectra with Overlapping Bands

In the case of two or more large overlapping bands, one must be careful in the estimates of the peak wavenumber and of the full-width-at-half-maximum intensity of each band. This is necessary because, for each band, the search for the wavenumbers at which these points occur, in the approximate k-spectrum, is within the wavenumber domain that is centered at the estimated peak absorption wavenumber and extends on either side of it to the estimated full-width-at-half-maximum intensity. One should not allow the search for these wavenumbers for a band to extend into a wavenumber domain where absorptions attributable to other bands are noticeable. A complete listing of the program input parameters and their formats appears at the beginning of the large MAIN segment of SKKTRANS.

## 3.0 DETERMINATION OF THE OPTICAL CONSTANTS OF A DIELECTRIC THIN FILM ON A METAL SUBSTRATE FROM REFLECTANCE MEASUREMENTS OF A SINGLE-FILM THICKNESS

In the past, most observers have used reflectance measurements of films to compute the optical constants n and k of a film material by noting, at a given wavenumber $\nu$, how the

reflectance varies with film thickness. (See, for example, Section 4.0 and Ref. 26.) This method is especially useful when the optical properties of the film material are known not to change with film thickness, and the reflectance data are available for at least two values of the film thickness.

If, however, the optical constants depend on film thickness, or when reflectance data for just one film thickness are available, one must find the constants in another way. In Section 2.0, a dispersion analysis of the transmittance of a single dielectric thin film on a thick substrate is given which yielded the n- and k-spectra of the dielectric and showed that the n-and k-spectra of $N_2/CO_2$ films, on 20-K Ge, vary in a nonrandom way upon the film thickness. At the core of that analysis was the calculation of the phase change $\phi$ suffered by the transmitted beam using a dispersion relation between $\phi$ and the modulus of the complex transmission coefficient. The phase change is of interest for its own sake, and the recovery of the phase change from intensity data constitutes the phase retrieval problem (Refs. 27 through 30).

A corresponding analysis of reflectance data has some complications not found in the transmittance analysis, primarily because the reflectance can be zero under certain conditions, whereas in principle the transmittance can never be. The possibility of zero reflectances introduces additional terms into the usual dispersion relations which increase the computational effort needed to use the single-film thickness method (Refs. 7 and 31 through 35).

## 3.1 THEORY

Figure 8 depicts the geometry of the theoretical model. A semi-infinite beam of monochromatic radiation is normally incident, in a medium of index $\hat{n}_0$ upon a thin film, index $n_1$. The film is sandwiched between the semi-infinite media having indices $\hat{n}_0$ and $\hat{n}_2$, and the interfaces are plane-parallel and infinite in extent.

In a typical experiment, the incident medium is very nearly a vacuum ($\hat{n}_0 = 1$), and the medium of index $\hat{n}_2$ is a metal substrate. One is able to consider the metal substrate as semi-infinite because $|\hat{n}_2|$ is much greater than unity for IR and visible radiation, and, hence, essentially no reflected waves exist in the metal substrate if it is sufficiently thick.

The geometry of a typical experiment usually does not allow the detection of beams that are actually normal to the interfaces, and a researcher must use beams that have nearly normal incidence. If the maximum angle of incidence of a ray in the beam is less than 10 deg or so, an observer frequently does not have to distinguish between the components of the beam which are parallel to the plane of incidence and those which are perpendicular to it (Ref. 36).

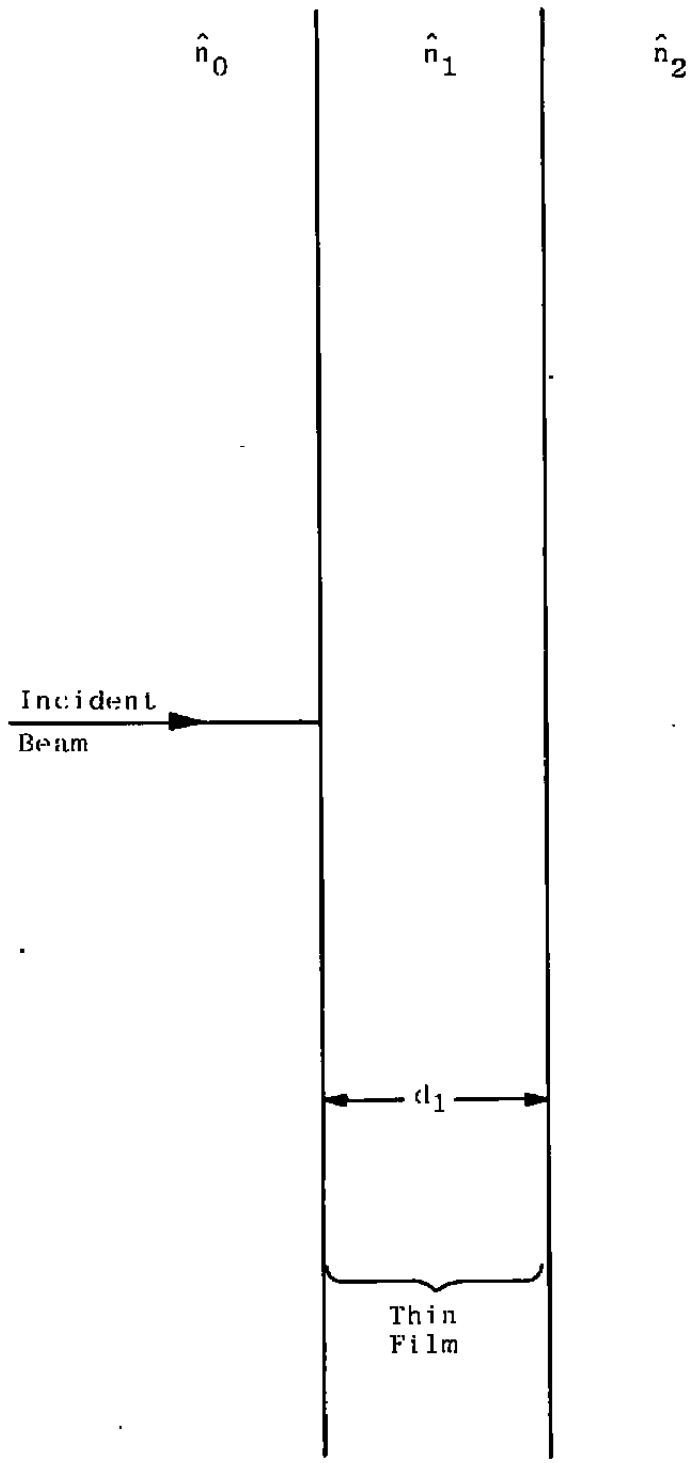


**Figure 8. Geometry depicting the analytical model for a thin film sandwiched between two semi-infinite media.**

### 3.1.1 Absolute Reflectance $R_{012}$

At a given wavenumber, the ratio of the intensity of the reflected beam to that of the incident beam is the experimental absolute reflectance $R_{012}$. Theoretically, the model in Fig. 8 gives $R_{012}$ as

$$R_{012}(\nu) = \hat{r}^*_{012}(\nu)\hat{r}_{012}(\nu) \tag{34}$$

where

$$\hat{r}_{012} = [\hat{r}_{01} + \hat{r}_{12}\exp(2i\hat{\gamma}_1 d_1)]/[1 + \hat{r}_{01}\,\hat{r}_{12}\exp(2i\hat{\gamma}_1 d_1)] \tag{35}$$

is Eq. (6), if the "0" and "2" subscripts are interchanged. At normal incidence, the complex reflection coefficient $\hat{r}_{jm}$ for radiation incident in medium j at the interface with medium m is given in Eq. (4), $\hat{\gamma}_1$ is defined in Eq. (8), and $d_1$ is the film thickness (Section 2.0 and Refs. 5, 7, 37, and 38). Please note that some authors define $\hat{r}_{jm}$ as the negative of the right-hand side of Eq. (4), and the two definitions differ by a phase of $\pm\pi$. (For examples, see Refs. 6, 7, and 25.)

### 3.1.2 Relative Reflectance R

In many experiments, it is often easier to measure the reflectance of an optical system relative to a standard reflectance rather than its absolute reflectance. The reflectance R of the vacuum-film-metal system relative to the vacuum-metal system reflectance is defined as

$$R = \frac{I_R}{I_{RS}} = \frac{I_R/I_0}{I_{RS}/I_0} = \frac{R_{012}}{R_{02}} \tag{36}$$

$I_R$ and $I_{RS}$ are the reflected beam intensities from the vacuum-metal systems, respectively, $I_0$ is the incident beam intensity, and $R_{02}$ is the absolute reflectance of the vacuum-metal system. Note that R can be greater than unity. Values of the complex index $\hat{n}_2$ of the metal can come from measured values of $R_{02}$, and how this might be done is illustrated in the next two sections.

### 3.1.3 Absolute Reflectance $R_{02}$ of the Vacuum-Metal Interface

For the case of a bare metal substrate, the theoretical model yields

$$R_{02}(\nu) = \hat{r}^*_{02}(\nu)\hat{r}_{02}(\nu) \tag{37}$$

for the absolute reflectance at the vacuum-metal interface, and the corresponding complex reflection coefficient is

$$\hat{r}_{02} = (\hat{n}_0 - \hat{n}_2)/(\hat{n}_0 + \hat{n}_2) \tag{38}$$

In an experiment, an observer often fits the experimental $R_{02}$ values to a function of the wavenumber, such as a polynominal. For instance, Arnold et al. (Ref. 26) found

$$R_{02}(\nu) = 0.939 - (4.25 \times 10^{-5}\ \text{cm})\nu \tag{39}$$

to be a good fit to the empirical data for the absolute reflectance of a vacuum-aluminum interface in the infrared. There are, however, certain theoretical restrictions on the mathematical form of $R_{02}(\nu)$, which Eq. (39) does not meet, and these are taken up in Section 3.2.2.

### 3.1.4 Evaluation of $\hat{n}_2$ from $R_{02}$

A researcher must know the complex refractive index of the metal, $\hat{n}_2$, before the film index $\hat{n}_1$ can be found from reflectance data because it is necessary to compute the reflection coefficient of the film-metal interface, $\hat{r}_{12}$, in any scheme for getting $\hat{n}_1$. [See Eqs. (4) and (35).] One method for obtaining the metal index $\hat{n}_2$ is through a Kramers-Kronig (KK), or a subtractive Kramers-Kronig (SKK), dispersion analysis of the observed vacuum-metal reflectance spectrum, $R_{02}(\nu)$. Two computer programs, KKR and SKKR, have been written which, respectively, perform KK and SKK analyses upon a reflectance spectrum to extract the optical constants of the reflecting medium.

Another way to calculate the complex index $\hat{n}_2$ of the metal comes by solving Eq. (38) for $\hat{n}_2$, which yields

$$\hat{n}_2 = \hat{n}_0(1 - \hat{r}_{02})/(1 + \hat{r}_{02}) = \hat{n}_0\,[1 - R_{02}^{1/2}\exp(i\beta_{02})]/[1 + R_{02}^{1/2}\exp(i\beta_{02})] \tag{40}$$

where, from Eq. (37), $\hat{r}_{02}$ is

$$\hat{r}_{02} = |\hat{r}_{02}|\exp(i\beta_{02}) = R_{02}^{1/2}\exp(i\beta_{02}) \tag{41}$$

The phase $\beta_{02}$ is the difference between the phase of the beam reflected at a vacuum-metal interface to that of the incident beam at the interface and is often difficult to determine empirically.

If $\beta_{02}$ cannot be measured directly, then good estimates of it can frequently be made. Because $|\hat{n}_2|$ is much greater than $|\hat{n}_0|$, which is unity for a true vacuum, the complex reflection coefficient $\hat{r}_{02}$ is nearly $-1$ making $\beta_{02}$ approximately equal to $\pi$. This has led many authors, Arnold et al. (Ref. 26), for example, to simply set $\beta_{02}$ to $\pi$ throughout their data range.

$\beta_{02}$ is not a constant function of the wavenumber, and, furthermore, if $\beta_{02}$ is set to $\pi$ and $\hat{n}_0$ to unity, Eq. (40) gives

$$\hat{n}_2 = n_2 + ik_2 = (1 + R_{02}^{1/2})/(1 - R_{02}^{1/2}) + i0 \tag{42}$$

Physically, this means $k_2$ of the metal is zero, and the metal medium would not absorb any of the radiation impinging upon it! In fact, a metal is a very highly absorbing medium over most of the IR and visible spectrum, and, for metals such as aluminum (Refs. 39 through 42), $k_2$ often exceeds $n_2$. At 8330 $cm^{-1}$, for instance, bulk Al has the optical constants $n_2 = 0.78$ and $k_2 = 9.16$ (Ref. 41).

The major problem in using Eq. (42) as an estimate of $\hat{n}_2$ is that sometimes this can introduce sizeable errors in the value of the reflection coefficient at the film-metal interface

$$\hat{r}_{12} = (\hat{n}_1 - \hat{n}_2)/(\hat{n}_1 + \hat{n}_2) = |\hat{r}_{12}| \exp(i\beta_{12}) \tag{43}$$

with

$$\beta_{12} = \tan^{-1}\left\{[(n + n_2)(k - k_2) + (n_2 - n)(k + k_2)] / [(n^2 - n_2^2) + (k^2 - k_2^2)]\right\} \tag{44}$$

and $\hat{n}_1 = n + ik$ for the film. If $k_2$ is set to zero, so that $\beta_{02}$ is $\pi$ and Eq. (42) gives $\hat{n}_2$, the phase change upon reflection at the film-metal interface, $\beta_{12}$, becomes a ficticious value

$$\beta'_{12} = \tan^{-1}[2n_2k/(n^2 - n_2^2 + k^2)] \tag{45}$$

In the spectral regions where the modulus of the film index of refraction, $|n_1|$, is much less than that of the metal, $|\hat{n}_2|$, both $\beta_{12}$ [Eq. (44)] and $\beta'_{12}$ [Eq. (45)] are approximately $\pi$ in value, and we can safely use Eq. (42). This situation is often encountered experimentally, and some authors set $\beta_{12}$ as well as $\beta_{02}$ to $\pi$ throughout their data domain (Ref. 26).

However, if either of the optical constants of the film of the metal become comparable in magnitude to one of the metal constants, some larger errors are possible. Suppose k and $k_2$ are approximately equal in a region of strong absorption by the film, but n is very small compared to $n_2$. The true value of $\beta_{12}$ is, from Eq. (44), $\beta_{12} \approx \tan^{-1}[2k/(-n_2)]$, which means $\beta_{12}$ is about 0.578 $\pi$ for the case $k = k_2 = 2n_2$. In contrast, if $\beta_{02}$ is set to $\pi$, and thus has a fictitious $k_2$ value of zero, $\beta_{12}$ from Eq. (45) is about $\tan^{-1}[2n_2k/(k^2 - n_2^2)]$, giving a fictitious value of about 0.295 $\pi$ when $k \cong 2n_2$. The discrepancy between these two values of $\beta_{12}$, 0.283 $\pi$, is large enough to cause a noticeable error in $\hat{r}_{12}$ and $\hat{r}_{012}$, if Eq. (42) is used to compute $\hat{n}_2$. Fortunately, instances in which k and $k_2$ are comparable rarely come up except in spectral regions where the film has strong absorptions.

There is a greater chance of error if one sets $\beta_{12}$ as well as $\beta_{02}$ to $\pi$. In the above example, for instance, the true value of $\beta_{12}$ is closer to ½ $\pi$ than $\pi$.

### 3.1.5 Multiple-Film Thickness Method

The model depicted in Fig. 8 and presented in Eqs. (34) through (44) is the basis of the method for finding the film optical constants at a given wavenumber by noting the change in the relative reflectance R as the film thickness varies. This multiple-film thickness method is valuable for films which do not change their optical properties with thickness and is discussed more fully in Section 4.0.

### 3.1.6 Single-Film Thickness Method

In cases where the optical constants of the film change with its thickness, or where there are reflectance data for a film material at only one thickness, one cannot apply the multiple-film thickness method of Section 4.0, because one seeks n and k at a given wavenumber and only one experimental piece of information exists, namely, R.

A second piece of information can be supplied from the use of any of the appropriate dispersion relations between the modulus of a complex quantity and its phase (Refs. 16 through 18, 22, and 43). Toll (Ref. 44) has shown that postulating the existence of dispersion relations for a linear system is equivalent to assuming that strict causality ("no output before input") holds for the system.

In the present instance, one can find the modulus of the reflection coefficient $\hat{r}_{012}$ of the vacuum-film-metal system directly from experiment by using

$$|\hat{r}_{012}| = R_{012}^{1/2} = (R\, R_{02})^{1/2} \tag{46}$$

where

$$\hat{r}_{012} = |\hat{r}_{012}| \exp(i\phi) \tag{47}$$

where $\phi$ is the phase change upon reflection at the vacuum-film interface for a beam incident in the vacuum. The phase change $\phi$ is what is sought from a dispersion relation so that optical constants of the film, n and k, can be extracted by inversion of Eq. (35).

Lupashko et al. (Refs. 6 and 7) have derived the Kramers-Kronig (KK) dispersion relations for the special case in which a planar thin film is sandwiched between two transparent semi-infinite media. The following derivation of the KK relations of the vacuum-film-metal system is along the lines of Lupashko et al. (Ref. 7).

### 3.1.7 Derivation of the Kramers-Kronig (KK) Dispersion Relations for $\hat{r}_{012}$

In order to proceed, one must find and examine the analytic extension of the theoretical expansion for $\hat{r}_{012}(\nu)$ into the upper half of the complex wavenumber ($\hat{\nu}$) plane. A function $\hat{f}(\hat{z})$ that has a derivative relative to the complex number $\hat{z}$ at all points within a region of the $\hat{z}$-plane is an analytic function of $\hat{z}$ within that region (Refs. 45 through 47). The complex wavenumber is denoted by

$$\hat{\nu} = \nu_R + i\nu_I \tag{48}$$

#### 3.1.7.1 Extension of Optical Quantities into the Complex $\hat{\nu}$-Plane

Landau and Lifshitz (Refs. 22, 35, and 43) have demonstrated that in the upper half of the $\hat{\nu}$-plane, the extension of index $\hat{n}_j$ for material j has the following properties:

1. The $\hat{n}_j$ are analytic.
2. The values of $\hat{n}_j$ on either side of the positive imaginary axis are paired in the following way: $\hat{n}_j(-\hat{\nu}^*) = \hat{n}_j^*(\hat{\nu})$.
3. As $\hat{\nu}$ approaches infinity in any direction in the upper-half plane, $\hat{n}_j(\hat{\nu})$ approaches unity.
4. Along the positive imaginary axis, where $\hat{n}_j$ is real (Property 2), the values decrease monotonically from $\hat{n}_j$ (i0), which is greater than unity, to $\hat{n}_j(i\infty) = 1$ (Property 3).
5. The $\hat{n}_j$ are real only on the imaginary axis.

From a straightforward application of Property 2 to the extensions into the $\hat{\nu}$-plane of Eqs. (4), (8), and (35), respectively, it is found that in the upper-half plane (Ref. 43)

$$\hat{r}_{jm}(-\hat{\nu}^*) = \hat{r}_{jm}^*(\nu)$$

$$\hat{\gamma}_1(-\hat{\nu}^*) = -\hat{\gamma}_1^*(\hat{\nu})$$

and

$$\hat{r}_{012}(-\hat{\nu}^*) = \hat{r}_{012}^*(\hat{\nu}) \tag{49}$$

#### 3.1.7.2 Poles and Zeros of $\hat{r}_{012}(\hat{\nu})$

Dispersion relations can come from the real and imaginary parts of the closed contour integral $\oint_C \hat{S}(\hat{\nu})d\hat{\nu}/(\hat{\nu}^2 - \nu^2)$ (Refs. 7 and 35), which is zero if $\hat{S}(\hat{\nu})$ is analytic in the region contained within the closed path C lying in the upper half of the $\nu$-plane, i.e.,

$$\oint_C \hat{S}(\hat{\nu})d\hat{\nu}/(\hat{\nu}^2 - \nu^2) = 0 \tag{50}$$

if $\hat{S}$ is analytic within path C. It must be insured that C circumvents any poles of $\hat{S}$ as well as $\hat{\nu} = \pm\nu$ on the real axis.

In this case, $\hat{S}$ is chosen along the real axis to be

$$\hat{S}(\nu) = \ell n\, \hat{r}_{012}(\nu) = \ell n\, |\hat{r}_{012}(\nu)| + i\phi(\nu) \tag{51}$$

because interest is in the relationship between the modulus of $\hat{r}_{012}$, which can be measured, and its phase. The analytic extension of $\hat{S}$ into the upper-half plane is formally

$$\hat{S}(\hat{\nu}) = \ell n\, \hat{r}_{012}(\hat{\nu}) = \ell n\, |\hat{r}_{012}(\hat{\nu})| + i\phi(\hat{\nu}) \tag{52}$$

Equation (52) indicates that any pole or zero of $\hat{r}_{012}(\hat{\nu})$ is also a pole of $\hat{S}(\hat{\nu})$. However, there are no poles of $\hat{r}_{012}$ because, in the extension of Eq. (35), $|\hat{r}_{01}(\hat{\nu})\hat{r}_{12}(\hat{\nu}) \exp[2i\hat{\gamma}_1(\hat{\nu})d_1]|$ is less than unity everywhere in the upper-half plane (Ref. 7).

The zeros $\hat{\nu}_j$ of $\hat{r}_{012}(\hat{\nu})$ can be found by setting the extension of Eq. (35) to zero. With the aid of the extension of Eq. (8), the location of the zeros at $\hat{\nu} = \hat{\nu}_j$ are for

$$\begin{aligned}\hat{\nu}_j &= \ell n\left[-\hat{r}_{01}(\nu_j)/\hat{r}_{12}(\hat{\nu}_j)\right]/\left[4\pi i\, \hat{n}_1(\hat{\nu}_j)\, d_1\right] \\ &= \left\{\mathrm{Ln}\left[-\hat{r}_{01}(\hat{\nu}_j)/\hat{r}_{12}(\hat{\nu}_j)\right] + i \cdot 2p\pi\right\} \\ &\quad \Big/ \left\{4\pi i \hat{n}_1(\hat{\nu}_j) d_1\right\}\end{aligned} \tag{53}$$

The Ln function has the principal value of the natural logarithm function, $\ell n$, and p is any integer. Equation (53) is transcendental, so it cannot be solved for $\hat{\nu}_j$ directly. The relations are useful, though, in an iterative search for $\hat{\nu}_j$ (Section 3.2.3).

According to Eq. (49), if

$$\hat{\nu}_j = \nu_{Rj} + i\,\nu_{Ij} \tag{54}$$

is a zero of $\hat{r}_{012}$, $-\hat{\nu}_j^* = -\nu_{Rj} + i\nu_{Ij}$ is also a zero; that is, the zeros of $\hat{r}_{012}$ are reflected across the imaginary axis.

### 3.1.7.3 Evaluation of $\oint_C \hat{S}(\hat{\nu})d\hat{\nu}/(\hat{\nu}^2 - \nu^2) = 0$

The closed path of integration, C, (Fig. 9) is basically a quarter circle of radius L and the radial lines at each end of the arc which are along the positive real and imaginary axes. The path avoids the pole at $\hat{\nu} = \nu$ on the positive real axis with a semicircle of radius $\varrho$, and goes around a possible pole of $\hat{S}$ at $\hat{\nu} = i\hat{\nu}_{I0}$ on the positive imaginary axis with a semicircle of radius $\varrho_0$. There are cuts $\gamma_j$ and $\gamma_j'$ and small circles of radius $\varrho_j$ about the Z zeros $\nu_j$ of $\hat{r}_{012}$, not on the imaginary axis, which are also poles and branch points of $\hat{S}$. This choice of path C makes $\hat{S}(\hat{\nu})/(\hat{\nu}^2 - \nu^2)$ analytic within it. Thus, Eq. (50) may be used, which is

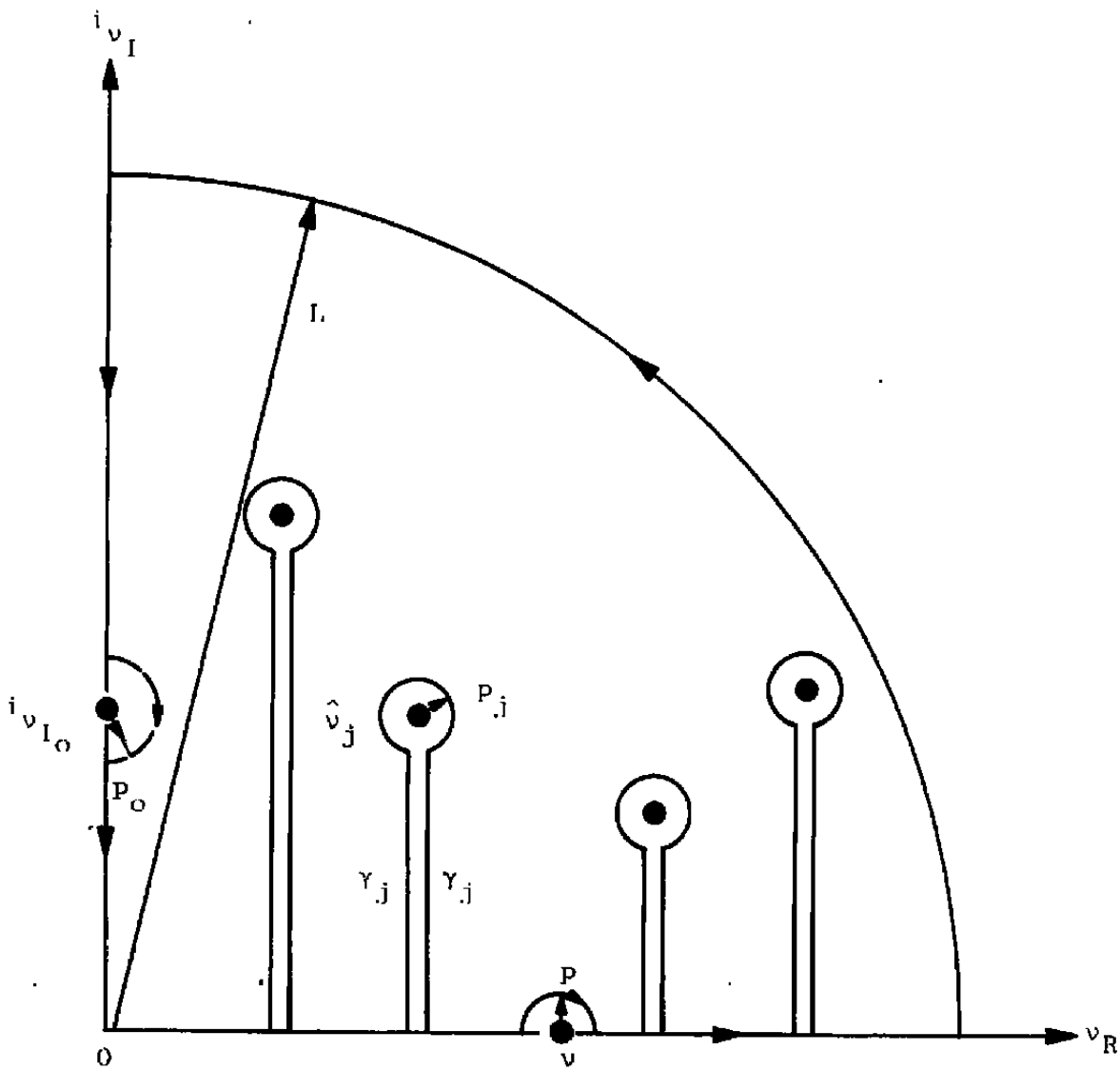


**Figure 9. Path C of contour integration $\oint_C \hat{S}(\hat{\nu})d\hat{\nu}/(\hat{\nu}^2 - \nu^2)$.**

$$0 = \int_0^{\nu-\varrho} \frac{\hat{S}(\nu_R)d\nu_R}{\nu_R^2 - \nu^2} + \int_{\nu+\varrho}^{L} \frac{\hat{S}(\nu_R)d\nu_R}{\nu_R^2 - \nu^2} + \int_{\alpha=\pi}^{\alpha=0} \frac{\hat{S}[\nu + \varrho\exp(i\alpha)]d[\varrho\exp(i\alpha)]}{[\nu + \varrho\exp(i\alpha)]^2 - \nu^2}$$

$$+ \sum_{j=1}^{Z} \left\{ \int_{\gamma_j} \frac{\hat{S}(\gamma_j)d(i\nu_I)}{(\nu_{Rj} + i\nu_I)^2 - \nu^2} + \int_{\gamma_j'} \frac{\hat{S}(\gamma_j')d(i\nu_I)}{(\nu_{Rj} + i\nu_I)^2 - \nu^2} \right.$$

$$\left. + \int_{\alpha_j=2\pi}^{\alpha_j=0} \frac{\hat{S}[\hat{\nu}_j + \varrho_j \exp(i\alpha_j)]d[\varrho_j\exp(i\alpha_j)]}{[\hat{\nu}_j + \varrho_j\exp(i\alpha_j)]^2 - \nu^2} \right\}$$

$$+ \int_{\theta=0}^{\theta=\pi/2} \frac{\hat{S}[L\exp(i\theta)]d[L\exp(i\theta)]}{[L\exp(i\theta)]^2 - \nu^2}$$

$$+ \int_{\nu_{I0}+\varrho_0}^{L} \frac{\hat{S}(i\nu_I)d(i\nu_I)}{\nu_I^2 + \nu^2} + \int_{\nu_{I0}-\varrho_0}^{0} \frac{\hat{S}(i\nu_I)d(i\nu_I)}{\nu_I^2 + \nu^2}$$

$$+ \int_{\alpha_0=\pi/2}^{\alpha_0=-\pi/2} \frac{\hat{S}[i\nu_{I0} + \varrho_0\exp(i\alpha_0)]d[\varrho_0 \exp(i\alpha_0)]}{[i\nu_{I0} + \varrho_0\exp(i\alpha_0)]^2 - \nu^2} \tag{55}$$

If no zero of $\hat{r}_{012}$ appears on the positive imaginary axis, the last three integrals on the right-hand side of Eq. (55) are combined into a single term:

$$\int_0^L \frac{\hat{S}(i\nu_I)d(i\nu_I)}{\nu_I^2 + \nu^2}$$

Now proceed to simplify Eq. (55) by reducing $\varrho$ and all $\varrho_j$ to zero and letting L approach infinity.

The sum of the integrals may be written along path segments $\gamma_j$ and $\gamma_j'$ as $\varrho_j$ goes to zero as

$$\int_{\gamma_j} \frac{\hat{S}(\gamma_j)d(i\nu_I)}{(\nu_{Rj} + i\nu_I)^2 - \nu^2} + \int_{\gamma_j'} \frac{\hat{S}(\gamma_j')d(i\nu_I)}{(\nu_{Rj} + i\nu_I)^2 - \nu^2}$$

$$= -i \int_0^{\nu_{Ij}} \frac{\Delta\hat{S}_j d\nu_I}{(\nu_{Rj} + i\nu_I)^2 - \nu^2}$$

$$= -i\Delta\hat{S}_j \int_0^{\nu_{Ij}} \frac{(\nu_{Rj}^2 - \nu^2 - \nu_I^2 - 2i\nu_{Rj}\nu_I)d\nu_I}{\nu_I^4 + 2(\nu_{Rj}^2 + \nu^2)\nu_I^2 + (\nu_{Rj}^2 - \nu^2)^2}$$

$$= \frac{-i\Delta\hat{S}_j}{2\nu} \left\{ \tan^{-1}\frac{\nu_{Ij}}{\nu_{Rj} - \nu} - \tan^{-1}\frac{\nu_{Ij}}{\nu_{Rj} + \nu} \right.$$

$$\left. - \frac{i}{2}\ln\left[\frac{\nu_I^2 + (\nu_{Rj} - \nu)^2}{\nu_{Ij} + (\nu_{Rj} + \nu)^2} \cdot \frac{(\nu_{Rj} + \nu)^2}{(\nu_{Ij} - \nu)^2}\right]\right\} \tag{56}$$

The quantity $\Delta\hat{S}_j = \hat{S}(\gamma_j') - \hat{S}(\gamma_j)$ is the value of $\hat{S}$ at a point on $\gamma_j'$ minus the value of $\hat{S}$ at the corresponding point on $\gamma_j$. In general, $\Delta\hat{S}_j$ is not zero because of the excursion of path C about the branch point $\hat{\nu}_j$, although, in our case, $\Delta\hat{S}_j$ is a constant value (see Section 3.1.7.4) and we can remove it from the integrand.

In the limit as all $\varrho_j$ go to zero, the integrals about all of the branch points of $\hat{S}$ are zero, i.e.,

$$\lim_{\varrho_j \to 0} \int_{\alpha_j} \frac{\hat{S}[\nu_j + \varrho_j\exp(i\alpha_j)]d[\varrho_j\exp(i\alpha_j)]}{[\nu_j + \varrho_j\exp(i\alpha_j)]^2 - \nu^2} = 0,\ j = 0, 1, 2, \ldots, Z \tag{57}$$

because $\hat{S}$ is only logarithmically infinite at $\hat{\nu} = \hat{\nu}_j$ (Ref. 35).

The limit about the pole $\hat{\nu} = \nu$ is taken as $\varrho$ approaches zero and L gets infinitely large:

$$\lim_{\varrho \to 0} \int_{\alpha} \frac{\hat{S}[\nu + \varrho\exp(i\alpha)]d[\varrho\exp(i\alpha)]}{[\nu + \varrho\exp(i\alpha)]^2 - \nu^2} = i\int_{\pi}^{0} \lim_{\varrho \to 0} \frac{\hat{S}[\nu + \varrho\exp(i\alpha)]}{2\nu + \varrho\exp(i\alpha)} d\alpha$$

$$= -\frac{i\pi S(\nu)}{2\nu} \tag{58}$$

and that of the sum of the first two integrals in Eq. (55):

$$\lim_{\substack{\varrho \to 0 \\ L \to \infty}} \left[\int_0^{\nu - \varrho} \frac{\hat{S}(\nu_R)d\nu_R}{\nu_R^2 - \nu^2} + \int_{\nu + \varrho}^{L} \frac{\hat{S}(\nu_R)d\nu_R}{\nu_R^2 - \nu^2}\right] = P\int_0^{\infty} \frac{\hat{S}(\nu_R)\,d\nu_R}{\nu_R^2 - \nu^2} \tag{59}$$

P indicates the Cauchy principal value of the integral.

Equations (56) through (59) are incorporated when Eq. (55) is rewritten for infinitesimally small $\varrho$ and $\varrho_j$ values and infinitely large L values as

$$0 = \bar{P} \int_0^\infty \frac{\hat{S}(\nu_R)d\nu_R}{\nu_R^2 - \nu^2} - \frac{i\pi\hat{S}(\nu)}{2\nu}$$

$$- \frac{i}{2\nu} \sum_{j=1}^{N} \Delta\hat{S}_j \left\{ \tan^{-1} \frac{\nu_{Ij}}{\nu_{Rj} - \nu} - \tan^{-1} \frac{\nu_{Ij}}{\nu_{Rj} + \nu} \right.$$

$$\left. - \frac{i}{2} \ln \left[ \frac{\nu_{Ij}^2 + (\nu_{Rj} - \nu)^2}{\nu_{Ij}^2 + (\nu_{Rj} + \nu)^2} \cdot \frac{(\nu_{Rj} + \nu)^2}{(\nu_{Rj} - \nu)^2} \right] \right\}$$

$$+ \lim_{L \to \infty} i \int_0^{\pi/2} \frac{\hat{S}[L\exp(i\theta)]d\theta}{L\exp\{(i\theta) - \nu^2/[L\exp(i\theta)]\}} + i \int_0^\infty \frac{\hat{S}(i\nu_I)d\nu_I}{\nu_I^2 + \nu^2} \tag{60}$$

### 3.1.7.4 Case $\hat{S}(\hat{\nu}) = \ln \hat{r}_{012}(\hat{\nu})$

In this section, Eq. (60) is evaluated for the choice of $\hat{S}$, namely,

$$\hat{S}(\hat{\nu}) = \ln \hat{r}_{012}(\hat{\nu})$$

The change in the value of $\hat{S}$ along the circular paths about the branch points $\hat{\nu}_j$ is

$$\Delta\hat{S}_j = \hat{S}(\gamma_j') - \hat{S}(\gamma_j) = -2\pi i \tag{61}$$

for j = 1, 2, ..., Z. The negative sign indicates the clockwise route of the integration path about $\hat{\nu}_j$.

The integral about the quarter circle of radius L depends on the limit of the integrand as L goes to infinity. Along the real axis the asymptotic behavior of index n of any material is, by Eq. (23) for very large $\nu_R$,

$$\hat{n}(\nu_R) \approx -\nu_p^2/(2\nu_R)^2 + \ldots \tag{62}$$

where $\nu_p$ is the "plasma wavenumber" defined in Eq. (24). Substituting Eq. (62) into Eqs. (4) and (8) and placing that result into Eq. (35), the asymptotic expression of $\hat{r}_{012}$ for large $\nu_R$ is

$$\hat{r}_{012}(\nu_R) \approx \left[ \nu_{p1}^2 + (\nu_{p2}^2 - \nu_{p1}^2)\exp(i4\pi\nu_R d_1) + \ldots \right] / (4\nu_R^2) \tag{63}$$

Here, as elsewhere in this report, the subscripts 0, 1, and 2 refer to the corresponding media in Fig. 8.

The analytic extension of Eq. (63) is used to calculate the limit of the integrand $\hat{S}[\mathrm{Lexp}(i\theta)]/\{\mathrm{Lexp}(i\theta) - \nu^2/[\mathrm{Lexp}(i\theta)]\}$ for infinitely large L. This is (Ref. 44)

$$\lim_{L\to\infty} \frac{\ln \hat{r}_{012}[\mathrm{Lexp}(i\theta)]}{\mathrm{Lexp}(i\theta)} = \lim_{L\to\infty} \frac{\ln[\nu_{pl}^2/(4L^2)] - 2i\theta}{\mathrm{Lexp}(i\theta)}$$

$$= 2\exp(-i\theta) \lim_{L\to\infty} L^{-1} \ln L^{-1}$$

$$= 0$$

Hence, the integral along the arc at infinity is zero, i.e.,

$$\lim_{L\to\infty} i \int_0^{\pi/2} \frac{S[\mathrm{Lexp}(i\theta)]d\theta}{\mathrm{Lexp}(i\theta) - \nu^2/[\mathrm{Lexp}(i\theta)]} = 0 \tag{64}$$

All that remains to evaluate in Eq. (6) is the integral along the positive imaginary axis. To do this one must know the behavior of $\hat{r}_{012}$ on the imaginary axis.

From the discussion in Section 3.1.7.1 it is known that $\hat{n}_0$, $\hat{n}_1$, $\hat{n}_2$, $\hat{r}_{01}$, $\hat{r}_{12}$, and $\hat{\gamma}_l$ are real everywhere on the positive imaginary axis, and hence, by Eqs. (8) and (35), so is $\hat{r}_{012}$. Also known is that $\hat{n}_0$ is unity everywhere, and $\hat{n}_1(i\nu_l)$ and $\hat{n}_2(i\nu_l)$ are greater than unity for finite positive $\nu_l$. This means

$$-1 < \hat{r}_{01}(i\nu_l) < 0, \text{ if } 0 \le \nu_l < \infty \tag{65}$$

On the other hand, $\hat{r}_{12}(i\nu_l)$ can have either sign depending on the difference $\hat{n}_1(i\nu_l) - \hat{n}_2(i\nu_l)$.

It is also true that

$$\exp[2i\hat{\gamma}_1(i\nu_l)d_1] = \exp[-4\pi d_1\hat{n}_1(i\nu_l)\nu_l] \le 1, \tag{66}$$

if $\nu_l \ge 0$.

These relations are sufficient to indicate the behavior of $\hat{r}_{012}$ on the positive imaginary axis. At the origin ($\hat{\nu} = i0$), the metal index $\hat{n}_2$ is infinite (Refs. 22 and 43), and $\hat{r}_{12}(i0)$ and $\hat{r}_{012}(i0)$ are both equal to $-1$, i.e.,

$$\hat{r}_{12}(i0) = \hat{r}_{012}(i0) = -1 \tag{67}$$

At infinitely large $\nu_I$, the indices approach unity (Property 3 of Section 3.1.7.1), and

$$\hat{r}_{012}(i\infty) = 0 \tag{68}$$

If $\hat{n}_1(i\nu_I)$ is always less than $\hat{n}_2(i\nu_I)$, and $\hat{r}_{12}(i\nu)$ and $\hat{r}_{012}(i\nu_I)$ never become positive, then no finite zero of $\hat{r}_{012}$ can exist on the positive imaginary axis. This case of no zeros seems very likely because while $\hat{n}_1$ has a finite value at the origin, $\hat{n}_2$ is infinite there, and both indices decrease monotonically to unity as $\nu_I$ approaches infinity (Property 4). Even if $\hat{n}_1$ should become greater than $\hat{n}_2$ somewhere on the imaginary axis, making $\hat{r}_{12}$ positive at that point, $\hat{r}_{012}$ will remain negative as the distance is increased from the origin until $\hat{r}_{01}$ is the negative or $\hat{r}_{12}\exp(-4\pi\nu_I d_1\hat{n}_1)$, which would occur at the first zero point, $\hat{\nu} = i\nu_{I0}$. Other zero points may appear even further from the origin with $\hat{r}_{012}$ alternating in sign in adjacent intervals between zeros. In any case, the number of zeros on the imaginary axis should be very few because $\hat{n}_2$ is usually greater than $\hat{n}_1$, and for sufficiently large $\nu_I$, the exponential decay will dominate $\hat{r}_{12}\exp(-4\pi\nu_I d_1\hat{n}_1)$.

If the only finite zero of $\hat{r}_{012}$ on the positive imaginary axis occurs at $\nu = i\nu_{I0}$, it can be written

$$\hat{r}_{012}(i\nu_I) = \begin{cases} -\left|\hat{r}_{012}(i\nu_I)\right|, & \text{for } 0 \le \nu_I \le \nu_{I0} \\ \left|\hat{r}_{012}(i\nu_I)\right|, & \text{for } \nu_I > \nu_{I0} \end{cases} \tag{69}$$

and the integral in Eq. (60) along the imaginary axis is

$$i\,P\int_0^\infty \frac{\hat{S}(i\nu_I)d\nu_I}{\nu_I^2 + \nu^2} = i\,P\int_0^\infty \frac{\ln\left|\hat{r}_{012}(i\nu_I)\right| d\nu_I}{\nu_I^2 + \nu^2} - \frac{\pi}{\nu}\tan^{-1}\frac{\nu_{I0}}{\nu} \tag{70}$$

It turns out that if the only zero of $\hat{r}_{012}$ on the imaginary axis is the one always present at infinity [Eq. (68)], then the same answer will be derived as when $\nu_{I0} = \infty$ is substituted into Eq. (70). In that instance, the arctangent term is $-\pi^2/(2\nu)$. If there are two or more finite zeros of $\hat{r}_{012}$ on the positive imaginary axis, each zero contributes an analogous arctangent term which alternates in sign in ascending $\nu_I$.

Now the desired relations, Eqs. (61), (64), and (70), can be written for Eq. (60) for the case $\hat{S} = \ln\hat{r}_{012}$. When these relations are used, Eq. (60) is

$$0 = P \int_0^\infty \frac{\ln|\hat{r}_{012}(\nu_R)|\,d\nu_R}{\nu_R^2 - \nu^2} + iP \int_0^\infty \frac{\phi(\nu_R)d\nu_R}{\nu_R^2 - \nu^2}$$

$$- \frac{i\pi \ln|\hat{r}_{012}(\nu)|}{2\nu} + \frac{\pi\phi(\nu)}{2\nu}$$

$$- \frac{\pi}{\nu} \sum_{j=1}^{Z} \left\{ \tan^{-1} \frac{\nu_{Ij}}{\nu_{Rj} - \nu} - \tan^{-1} \frac{\nu_{Ij}}{\nu_{Rj} + \nu} \right.$$

$$\left. - \frac{i}{2} \ln \left[ \frac{\nu_{Ij}^2 + (\nu_{Rj} - \nu)^2}{\nu_{Ij}^2 + (\nu_{Rj} + \nu)^2} \cdot \frac{(\nu_R + \nu)^2}{(\nu_R - \nu)^2} \right] \right\} +$$

$$+ iP \int_0^\infty \frac{\ln|\hat{r}_{012}(i\nu_I)|\,d\nu_I}{\nu_I^2 + \nu^2} - \frac{\pi}{\nu} \tan^{-1} \frac{\nu_{I0}}{\nu} \tag{71}$$

### 3.1.7.5 Kramers-Kronig Dispersion Relation for $\phi(\nu)$

The solution of the real part of Eq. (71) for the phase $\phi$ of $\hat{r}_{012}$ is the Kramers-Kronig (KK) relation

$$\phi(\nu) + 2m\pi = \frac{-2\nu}{\pi} P \int_0^\infty \frac{\ln|\hat{r}_{012}(\nu_R)|\,d\nu_R}{\nu_R^2 - \nu^2}$$

$$+ 2 \sum_{j=1}^{N} \left( \tan^{-1} \frac{\nu_{Ij}}{\nu_{Rj} - \nu} - \tan^{-1} \frac{\nu_{Ij}}{\nu_{Rj} + \nu} \right)$$

$$- 2 \tan^{-1} \frac{\nu_{I0}}{\nu} \tag{72}$$

m is an integer, and the addition of a multiple of $2\pi$ to Eq. (72) does not affect $\exp(i\phi)$. Zeros of $\hat{r}_{012}$ occur at $\hat{\nu}_j = \nu_{Rj} + i\nu_{Ij}$, where $\nu_{Rj}, \nu_{Ij} \geq 0$, and at $\nu = i\nu_{I0}$, at which $\nu_{I0}$ may be infinite. Ordinarily the KK relation is used to find $\phi$ from the measured values of the relative reflectance R, and for these situations, one substitutes Eq. (46), $|\hat{r}_{012}| = (R\,R_{02})^{1/2}$, into Eq. (72).

There are several items to keep in mind when applying Eq. (72) to experimental data. If there are no finite zeros of $\hat{r}_{012}$ on the positive imaginary axis, the substitution $\nu_{I0} = \infty$ gives $-\pi$ for $-2\tan^{-1}\nu_{I0}/\nu$. If there is a multiple number of zeros $\nu_{0\ell}$, where $\nu_{0\ell-1}$ is less than $\nu_{0\ell}$ along the positive imaginary axis, the summation $2\,\Sigma(-1)^{\ell}\tan^{-1}\nu_{0\ell}/\nu$ should replace $-2\tan^{-1}\nu_{I0}/\nu$.

One should also add $2\pi$ to the right-hand side of Eq. (72) for every $\nu_{Rj}$ that is less than $\nu$, if the principal value of the arctangent function is used.

### 3.1.8 Subtractive Kramers-Kronig (SKK) Relation for $\phi(\nu)$

The subtractive Kramers-Kronig (SKK) relation for $\phi$ depends upon the phase $\phi(\nu_0)$ found at $\nu = \nu_0$ directly from an experiment or computed from the equation

$$\phi(\nu_0) = \mathrm{Im}\left[\ln r_{012}(\nu_0)\right] \tag{73}$$

after one enters the values of the optical constants at $\nu_0$, determined in a separate experiment, into Eqs. (4), (8), and (35)(Ref. 19). Usually an experimenter chooses $\nu_0$ to be in a transparent, or nearly transparent, region somewhere in the midst of the reflectance spectrum. As noted before, Ahrenkiel (Ref. 19) has shown the SKK relation to be less sensitive than the corresponding KK equation to errors introduced by the extrapolations of the data which must be made outside the data range.

#### 3.1.8.1 Derivation of the SKK Relation

At the wavenumber $\nu_0$ at which $\phi$ is known, Eq. (72) is

$$\begin{aligned}\phi(\nu_0) + 2m\pi = {} & \frac{-2\nu_0}{\pi} P \int_0^{\infty} \frac{\ln\left|\hat{r}_{012}(\nu_R)\right| d\nu_R}{\nu_R^2 - \nu_0^2} \\ & + 2\sum_{j=1}^{Z}\left(\tan^{-1}\frac{\nu_{Ij}}{\nu_{Rj} - \nu_0} - \tan^{-1}\frac{\nu_{Ij}}{\nu_{Rj} + \nu_0}\right) \\ & - 2\tan^{-1}\frac{\nu_{I0}}{\nu_0}\end{aligned} \tag{74}$$

Equations (72) and (74) can be combined to obtain the SKK relation for $\phi(\nu)$ which is

$$\phi(\nu) + 2m\pi = \frac{2\nu(\nu_0^2 - \nu^2)}{\pi} P \int_0^\infty \frac{\ln|\hat{r}_{012}(\nu_R)|\, d\nu_R}{(\nu_R^2 - \nu^2)(\nu_R^2 - \nu_0^2)} + \frac{\nu}{\nu_0}\left[\phi(\nu_0) + 2m\pi\right]$$

$$+ 2\sum_{j=1}^{Z}\left[\tan^{-1}\frac{\nu_{Ij}}{\nu_{Rj} - \nu} - \tan^{-1}\frac{\nu_{Ij}}{\nu_{Rj} + \nu}\right.$$

$$\left. - \frac{\nu}{\nu_0}\left(\tan^{-1}\frac{\nu_{Ij}}{\nu_{Ij} - \nu_0} - \tan^{-1}\frac{\nu_{Ij}}{\nu_{Rj} + \nu_0}\right)\right]$$

$$- 2\left(\tan^{-1}\frac{\nu_{I0}}{\nu} - \frac{\nu}{\nu_0}\tan^{-1}\frac{\nu_{I0}}{\nu_0}\right) \tag{75}$$

As was done for the KK relation, Eq. (72) $(R\ R_{02})^{1/2}$ can be substituted for $|\hat{r}_{012}|$. All the considerations about possible zeros on the positive imaginary axis which apply to the KK relation, also apply to Eq. (75). They appear in 3.1.7.5.

## 3.2 LOCATION OF THE ZEROS OF $\hat{r}_{012}$

The dispersion relations for $\phi$, the phase of $\hat{r}_{012}$, are useless unless the zero points of $\hat{r}_{012}$ are known in the upper half of the $\hat{\nu}$-plane. There are some restrictions on the form that the zeros, $\hat{\nu}_j$, of $\hat{r}_{012}$ can have. For instance, in theory, zeros not on the imaginary axis always appear in pairs that are symmetric in position relative to the imaginary axis (Section 3.1.7.3).

In this section, methods are examined for estimating the location of the zeros of $\hat{r}_{012}(\hat{\nu})$. The general scheme is to estimate the functional form that optical quantities have on the real $(\nu_R)$ axis and to use the analytic extension of these forms into the complex $\hat{\nu}$-plane to compute the values of the optical quantities away from the real axis.

### 3.2.1 Finite Number of Zeros

Fortunately, the number of zeros of $\hat{r}_{012}$ is finite because of the forbidden wavenumber gap in solid dielectrics and semiconductors (Ref. 48). Near the gap the absorption index of the film greatly exceeds the refractive index, and the zeros of $\hat{r}_{012}$ cross into the lower half of the complex plane in the manner explained by Lupaskho et al. (Ref. 7).

### 3.2.2 Approximate Values of $\hat{n}_1$ and $\hat{n}_2$

Good approximation formulas must be available for the media indices $\hat{n}_0$, $\hat{n}_1$, and $\hat{n}_2$ if one hopes to find the zeros of $\hat{r}_{012}$. The assumption is made that medium 0 is a vacuum; hence, $\hat{n}_0(\hat{\nu})$ is unity for all complex wavenumbers $\hat{\nu}$. Thus, approximate functional forms only for the film and metal indices, $\hat{n}_1$ and $\hat{n}_2$, are sought.

In the preliminary work, the analytic extension of Eq. (40),

$$\hat{n}_2(\hat{\nu}) = [1 - \hat{r}_{02}(\hat{\nu})]/[1 + \hat{r}_{02}(\hat{\nu})] \tag{76}$$

was used to compute the metal index from the extension of an empirical relation for $\hat{r}_{02}$, such as Eq. (39),

$$\hat{r}_{02}(\hat{\nu}) = -[0.939 - (4.25 \times 10^{-5}\ \text{cm})\hat{\nu}]^{1/2} \tag{77}$$

Note that Eq. (77) does not satisfy the relation $\hat{r}_{02}(-\hat{\nu}^*) = \hat{r}_{02}^*(\nu)$ in Section 3.1.7.1, and the location of the zeros obtained from Eq. (77) are not paired as theory predicts in Section 3.1.7.2.

In the remainder of this section approximate expressions will be derived for the optical constants of the film, $n(\hat{\nu})$ and $k(\hat{\nu})$. First consider spectral domains where the film causes noticeable absorptions of radiation. In the actual wavenumber domains where the film is sufficiently absorbing, the film acts very much like a metal, $|\hat{r}_{01}|$ is much greater than $|\hat{r}_{12}\exp(2i\hat{\gamma}_1 d_1)|$, and Eqs. (4), (34), and (35) give

$$R_{012} \approx |\hat{r}_{01}|^2 = [(1 - n)^2 + k^2]/[(1 + n)^2 + k^2] \tag{78}$$

Solving Eq. (78) for k,

$$k \approx \left\{[R_{012}(1 + n)^2 - (1 - n)^2]/[1 - R_{012}]\right\}^{1/2} \tag{79}$$

from which an approximate k-spectrum can be constructed if crude estimates of n and experimental values of $R_{012}$, are obtained, perhaps, from Eq. (46) using measurements of the absolute reflectance R.

The estimates of the k- and n-spectra can be refined if Eqs. (21) and (79) are incorporated in an iterative process. In the first iteration n may be set to unity which makes Eq. (79) become

$$k \approx 2R_{012}^{1/2}/(1 - R_{012})^{1/2} \tag{80}$$

These k-values can be inserted into Eq. (21) to find an n -spectrum. Subsequent iterative steps can use Eqs. (21) and (79) to find updated k- and n-values.

There are two major reasons why a film in certain spectral regions may not be sufficiently absorbing enough to be represented by Eqs. (78), (79), or (80). First, the absorption coefficient k of the film medium may be too small for those wavenumbers. In those spectral ranges, setting k to zero and n to the $n_0$-value of Eq. (21) should give good results. The second reason for small film absorptions is that the film thickness $d_1$ is so small that $|\hat{r}_{12}\exp(2i\hat{\gamma}_1 d_1)$ is comparable to, or exceeds, $|\hat{r}_{01}|$ even though the k-values may be large for those wavenumbers. The construction of approximate k- and n-spectra is somewhat more difficult in those spectral domains because a researcher must make more assumptions about k and $d_1$. A test of Eqs. (79) and (80) was conducted with theoretical spectra, and results are discussed in Section 3.2.3.

As an approximation to the analytic extension of the index of the film, one can use

$$\hat{n}_1(\hat{\nu}) = [\hat{\epsilon}_1(\hat{\nu})]^{1/2} \tag{81}$$

where the dielectric constant of the film is (Ref. 31)

$$\hat{\epsilon}_1(\hat{\nu}) = \hat{\epsilon}_0 + \sum_{p=1}^{N} a_p(\nu_p^2 - \hat{\nu}^2 - ib_p\hat{\nu})^{-1} \tag{82}$$

It is noted that $\hat{\epsilon}_0$ and the positive constants $a_p$ and $b_p$ can be found from the approximate k-and n-spectra of Eqs. (79) and (21), by computing $\hat{\epsilon}_1(\nu)$ from

$$\hat{\epsilon}_1(\nu) = [n(\nu) + ik(\nu)]^2 \tag{83}$$

then fitting $\hat{\epsilon}_1(\nu)$ to the form that Eq. (82) has along the real axis, i.e., when $\hat{\nu} = \nu$.

### 3.2.3 Test of an Iterative Method to Find the Zeros

Equation (53) has been incorporated in an iterative method of locating the zeros of $\hat{r}_{012}$. For each value of the index j, the iterations are started by inserting into Eq. (53) the $\hat{r}_{01}$, $\hat{r}_{12}$, and $\hat{n}_1$ values computed at an initial guess $\nu_j(0)$ of the zero, $\hat{\nu}_j$, thus, getting a new value, $\hat{\nu}_j^{(1)}$. New values of $\hat{r}_{01}$, $\hat{r}_{12}$, and $\hat{n}_1$ at $\hat{\nu}_j^{(1)}$ are computed to reinsert into Eq. (53) for the second iteration. The iterations are repeated until the moduli of successive iterative $\hat{\nu}_j$ values differ by less than $10^{-12}$ or a maximum number of iterations is completed.

The method for convergence was tested using theoretical spectra for the film and metal indices $\hat{n}_1$ and $\hat{n}_2$.

A theoretical film index $\hat{n}_1$ was calculated from Eqs. (81) and (82). The choices for the parameters of Eq. (82) were $\epsilon_0 = 1.5 + i0$, $N = 2$ (the number of absorption bands), $a_1 = a_2 = 3.0 \times 10^5\ cm^{-2}$, $\nu_1 = 2000\ cm^{-1}$, $\nu_2 = 3000\ cm^{-1}$, and $b_1$ and $b_2 = 10\ cm^{-1}$. It is noted that $\hat{n}_2(\hat{\nu})$ was obtained from Eq. (76) by using relations similar to Eq. (77) for $\hat{r}_{02}(\hat{\nu})$.

In the test of the iterative algorithm, the initial guess $\nu(0)$ was set to be the origin, film thickness ($d_1$) values varied from a 0.1 to 10 $\mu$m, and the integer j progressed over the values 0, $\pm 1$, $\pm 2$, ..., until the converged value of $|\nu_{Rj}|$ exceeded 10000 $cm^{-1}$. Calculations were stopped there because zeros with real parts that are far from the data wavenumber range give a nearly constant contribution to the phase in Eqs. (72) and (75), and their exact locations would not be important in a typical experiment.

In nearly every instance, a converged value of $\hat{\nu}_j$ was found which, when substituted into the analytic extension of Eq. (35), yielded a value of $\hat{r}_{012}(\hat{\nu})$ whose real and imaginary parts differed from zero by less than $10^{-6}$. In one calculation, j was 0, and the convergence was not as good, but the computed zero was nearly identical to that for $j = -1$. In all of the other exceptional cases, the j-values were negative or zero, and the converged zero values were in the second quadrant or the lower half of the complex plane. Zeros in the first quandrant did not seem to be missing.

Theoretically, the zeros of $\hat{r}_{012}$ should appear in pairs reflected about the imaginary axis (Section 3.1.7.2), but, as was pointed out in Section 3.2.2, the use of an empiricial relation for $\hat{r}_{02}$, such as Eq. (77), will destroy this pairing. In fact, when Eq. (77) is used one obtains an approximate pairing of the zeros. However, when $\hat{r}_{02}(\hat{\nu}) \equiv -0.9$, so that $\hat{r}_{02}(-\hat{\nu}^*) = \hat{r}_{012}^*(\nu^*)$, the converged values of the zeros were paired according to $\hat{\nu}_j = -\hat{\nu}_{-j}^*$.

The same hypothetical spectra were also used to compare the approximations for the film absorption coefficient k [Eqs. (79) and (80)] to the theoretical values. For hypothetical film thicknesses 1 $\mu$m or greater, there was agreement to at least four significant digits of the theoretical k-values with the same values estimated by Eq. (79) in the strong absorption regions. Under the same conditions, the values found by Eq. (80) were within 30 percent of the theoretical values. As expected, the agreement worsened in weaker absorption regions or for smaller film thicknesses because the conditions under which Eqs. (79) and (80) were valid were not met (Section 3.2.2).

## 3.3 COMPUTER PROGRAM SKKREFL

The authors are now engaged in writing and testing computer program SKKREFL for the SKK analysis of experimental reflectance values of a single-film thickness when the beam is normally incident in a vacuum upon a thin film deposited on a metal substrate. The three major segments of the program, MAIN, KAMKON, and NLNSYS, are essentially the same as the corresponding segments of the program SKKTRANS which has successfully analyzed transmittance data for a single-film thickness (Section 2.2).

KAMKON does the numerical integration necessary to evaluate the SKK dispersion relation [Eq. (75)] for the phase $\phi$ of $\hat{r}_{012}$ at a given wavenumber.

NLNSYS uses the experimental value of $\hat{r}_{012}$ that KAMKON finds from Eqs. (46) and (47). It is identical to the segment of the same name in SKKTRANS, as is the coding needed to choose the most likely, or "best" pair of n- and k-values should the algorithms yield more than one pair (Section 2.2).

It may be necessary to revise the film optical constants, n and k, obtained from NLNSYS because the algorithm in MAIN which locates the zero points of $\hat{r}_{012}$ uses approximations to these constants. The program can use the n- and k-values found in NLNSYS in a search for revised zero locations and compare them with those found originally in MAIN. If a revision is necessary, SKKREFL can redo, one or more times, the steps in KAMKON and NLNSYS with updated data from the previous pass.

At present, program SKKREFL is not completely assembled or fully tested. However, many of its algorithms have worked successfully in other programs previously written, and the method of finding zeros of $\hat{r}_{012}$ has passed all of the tests to date.

# 4.0 THE MULTIPLE-FILM THICKNESS METHOD: PROGRAM RENLIN

Computer program RENLIN was written to analyze the normal reflectance of a beam incident upon a film deposited on a metal substrate over several film thicknesses. RENLIN yields the complex index of the film material, $\hat{n}_1$, which, it is assumed, does not depend on film thickness. The method of analysis is based on the model contained in Eqs. (4), (8), and (34) through (44). For the model, it is noted that at a certain wavenumber, the film indices n and k, and all other parameters, are constant by assumption during an experiment.

RENLIN fits the experimental reflectance values of two or more film thicknesses at a given wavenumber to the model of Eqs. (4), (8), and (34) through (44). The fitting procedure is the nonlinear least-squares algorithm of Marquardt (Ref. 8), and the fitted parameters are n and k of the film material. Except for the equations representing the model and some modifications of the data input procedures, RENLIN is identical in coding to TRNLIN, the program that fits experimental transmittance values of thin films used in Ref. 1. It is recommended that the present version of the nonlinear least-squares algorithm in program segment NLIN, which is a part of both of the RENLIN and TRNLIN programs, be revised. The coding of this algorithm is in single-precision arithmetic, whereas all the other algorithms use double precision. It also happens to be very confusing to follow. The main reason for the proposed revision of NLIN, however, is to improve its efficiency. Least-squares algorithms tend to be costly procedures involving minutes of CPU time and kilobytes of memory. Huber (Ref. 49) has recently discovered a new "extrapolated least-squares optimization" method that typically reduces the number of iterative steps to about half that of the conventional algorithms. The method is actually a slight modification of the present algorithm in NLIN and would improve each of the present iterative steps.

## 5.0 CONCLUSIONS

The lifetime of space satellites is often directly related to contamination of critical optical surfaces by condensed gas films. A basic property required for determining optical contamination effects is the complex refractive index of the gas film. Results of efforts to develop mathematical models and computer programs for the determination of the complex mathematical models and computer programs for the determination of the complex refractive index from optical transmittance and reflectance measurements are presented in this report.

In previous work (Ref. 1), the program TRNLIN has been used successfully to determine refractive index values using experimental transmittance data for multiple-film thicknesses of condensed gases. The program RENLIN has been written to analyze the normal reflectance of a beam incident on a film deposited on a metal substrate over several film thicknesses. RENLIN yields the complex index of the film material which is assumed not to depend on film thickness. Except for equations representing the reflectance model and some modifications of the data input procedures, RENLIN is identical in coding to TRNLIN.

Detailed descriptions of two new programs to determine the complex refractive index from experimental measurements of a single-film thickness are presented. The advantage of this model is that the assumption used in previous models that the optical properties of a dielectric film are independent of film thickness is not required. The program SKKTRANS utilizes a new subtractive Kramers-Kronig algorithm which gives highly reliable index values from measurements of the absolute transmittance of a single uniform thin film deposited on

a uniform thick substrate. This program reduces the number of necessary experimental measurements and is capable of noting any differences in the optical constants of the film material due to changes in film thickness. A theoretical $CO_2$-cryofilm transmittance spectrum was used to test the algorithms in SKKTRANS. Excellent agreement was found between calculated and original index values. From the results of the SKKTRANS program and the transmittance data taken previously from an $N_2/CO_2$ mixture, it was observed that the absorption index determined through the SKKTRANS program increased with thickness. Further investigation is required to determine whether this trend is a real physical effect or a computational artifact. This same effect was observed for other gas mixtures. The values computed for individual thickness using SKKTRANS were in close agreement with those obtained with TRNLIN and multiple-film thicknesses. Also the program SKKREFL was derived for determining n and k using subtractive Kramers-Kronig technique from experimental reflectance data for a single-film thickness. This program is not completely assembled and has not been fully tested.

## REFERENCES

1. Palmer, K. F., Roux, J. A., and Wood, B. E. "The Infrared Optical Properties of Mixtures of Molecular Species at 20 K." AEDC-TR-80-30 (AD-A094214), January 1981; also AIAA paper No. 83-1452.

2. Wood, B. E. and Roux, J. A. "Infrared Optical Properties of Thin $H_2O$, $NH_3$, and $CO_2$ Cryofilms." *Journal of the Optical Society of America*, Vol. 72, No. 6, June 1982, pp. 720-728.

3. Roux, J. A. and Wood, B. E. "Infrared Optical Properties of Solid Monomethyl Hydrazine, $N_2O_4$, and $N_2H_4$ at Cryogenic Temperatures." *Journal of the Optical Society of America*, Vol. 73, No. 9, September 1983, pp. 1181-1188.

4. Wood, B. E. and Roux, J. A. "IR Optical Properties of Thin CO, NO, $CH_4$, HCl, $N_2O$, $O_2$, $N_2$, and Ar Cryofilms." *American Institute of Aeronautics and Astronautics*, Aerospace Sciences Meeting, 21st, Reno, NV, January 10-13, 1983; also AIAA paper No. 83-0244.

5. Heavens, O. S. *Optical Properties of Thin Films*. Dover Publications, Inc., New York, 1965.

6. Lupashko, E. A., Miloslavskii, V. K., and Shklyarevskii, I. N. "Use of the Kramers-Kronig Dispersion Relations in Determining the Phase Shift Occurring upon Reflection of Light from Thin Dielectric Layers." *Optica i Spektroskpiya*, Vol. 24, No. 2, February 1968, pp. 257-262. (*Optics and Spectroscopy*, Vol. 24, No. 2, February 1968, pp. 132-134.)

7. Lupashko, E. A., Miloslavskii, V. K., and Shklyarevskii, I. N. "Use of the Kramers-Kronig Dispersion Relationships to Calculate the Phase of the Wave Reflected from Thin Dielectric Layers." *Optica i Spektroskpiya*, Vol. 29, No. 4, October 1970, pp. 789-793. (*Optics and Spectroscopy*, Vol. 29, No. 4, October 1970, pp. 419-422.)

8. Maeda, S., Thyagarajan, G., and Schatz, P. N. "Absolute Infrared Intensity Measurements in Thin films: II. Solids Deposited on Halide Plates." *Journal of Chemical Physics*, Vol. 39, No. 12, December 1963, pp. 3474-3481.

9. Harris, L., Beasley, J. K., and Loeb, A. L. "Reflection and Transmission of Radiation by Metal Films and the Influence of Nonabsorbing Backings." *Journal of the Optical Society of America*, Vol. 41, No. 9, September, 1951, pp. 604-614.

10. White, J. U. and Ward, W. M. "Effects of Interference Fringes in Infrared Absorption Cells." *Analytical Chemistry*, Vol. 37, No. 2, February, 1965, pp. 268-270.

11. Marquardt, D. W. "An Algorithm for Least-Squares Estimation of Nonlinear Parameters." *Journal of the Society for Industrial and Applied Mathematics*, Vol. 11, No. 2, June, 1963, pp. 431-441.

12. Bell, E. E. "Measurements of the Far-Infrared Optical Properties of Solids with a Michelson Interferometer Used in the Asymmetric Mode: Part I, Mathematical Formulation." *Infrared Physics*, Vol. 6, 1966, pp. 57-74; Russell, E. E. and Bell, E. E. "Measurements of the Far-Infrared Optical Properties of Solids with a Michelson Interferometer Used in the Asymmetric Mode: Part II, The Vacuum Interferometer." *Infrared Physics*, Vol. 6, 1966, pp. 75-84.

13. Gast, J. and Genzel, L. "An Amplitude Fourier Spectrometer for Infrared Solid State Spectroscopy." *Optics Communications*, Vol. 8, 1973, pp. 26-30.

14. Parker, T. J., Chambers, W. G., and Angress, J. F. "Dispersive Reflection Spectroscopy in the Far-Infrared by Division of the Field of View in a Michelson Interferometer." *Infrared Physics*, Vol. 14, 1974, pp. 207-215.

15. Eldridge, J. E. and Staal, P. R. "Far-Infrared Dispersive-Reflection Measurements on NaCl, Compared with Calculations Based on Cubic and Quartic Anharmonicity: I. Room Temperature." *Physical Revue B*, Vol. 16, 1977, p. 4608.

16. Peterson, C. W. and Knight, B. W. "Causality Calculations in the Time Domain: An Efficient Alternative to the Kramers-Kronig Method." *Journal of the Optical Society of America*, Vol. 63, No. 10, October, 1973, pp. 1238-1242.

17. Johnson, D. W. "A Fourier Series Method for Numerical Kramers-Kronig Analysis." *Journal of Physics A*, Vol. 8, No. 4, April, 1975, pp. 490-495.

18. King, F. W. "A Fourier Series Algorithm for the Analysis of Reflectance Data." *Journal of Physics C*, Vol. 10, No. 8, August, 1977, pp. 3199-3204.

19. Ahrenkiel, R. K. "Modified Kramers-Kronig Analysis of Optical Spectra." *Journal of the Optical Society of America*, Vol. 61, No. 12, December, 1971, pp. 1651-1655.

20. Peiponen, K. E. "On the Properties of the Complex Refractive Index of Lorentzian Type." *Physica Scripta*, Vol. 21, 1980, pp. 181-182.

21. Wooten, F. *Optical Properties of Solids*, Academic Press, New York, 1972.

22. Landau, L. D. and Lifshitz, E. M. *Electrodynamics of Continuous Media*, Pergamon Press, New York, 1960.

23. Ditchburn, R. W. *Light*, Academic Press, New York, 1976, 3rd Ed., Vols. 1 and 2.

24. Roux, J. A., Wood, B. E., and Smith, A. M. "IR Optical Properties of Thin $H_2O$, $NH_3$, $CO_2$ Cryofilms." AEDC-TR-79-57 (AD-A074913), September, 1979.

25. Smith, D. Y. and Manogue, C. A. "Superconvergence Relations and Sum Rules for Reflection Spectroscopy." *Journal of the Optical Society of America*, Vol. 71, No. 8, August, 1981, pp. 935-947.

26. Arnold, F., Sanderson, R. B., Mantz, A. W., and Thompson, S. B. "Infrared Spectral Reflectance of Plume Species on Cooled Low-Scatter Mirrors." AFRPL-TR-73-52, September 1973.

27. Burge, R. E., Fiddy, M. A., Greenaway, A. H., and Ross, G. "The Phase Problem." *Royal Society of London. Proceedings*, Vol. 350 A, 1976, pp. 191-212.

28. Hoenders, B. J. "On the Solution of the Phase Retrieval Problem." *Journal of Mathematical Physics*, Vol. 16, No. 9, September 1975, pp. 1719-1725.

29. Walther, A. "The Question of Phase Retrieval in Optics." *Optica Acta*, Vol. 10, No. 1, January 1963, pp. 41-49.

30. Roman, P. and Marathay, A. S. "Analyticity and Phase Retrieval." *Nuovo Cimento*, Vol. 30, No. 6, 16 December 1963, pp. 1452-1464.

31. Young, R. H. "Validity of the Kramers-Kronig Transformation Used in Reflection Spectroscopy." *Journal of the Optical Society of America*, Vol. 67, No. 4, April 1977, pp. 520-523.

32. Chambers, W. G. "Failures in the Kramers-Kronig Analysis of Power-Reflectivity." *Infrared Physics*, Vol. 15, No. 2, May 1975, pp. 139-141.

33. Filinski, I. and Skettrup, T. "Direct Determination of the Phase of Reflectivity in CdS and ZnO in the Exciton Region." *Solid State Communications*, Vol. 11, No. 12, December 1972, pp. 1651-1653.

34. Clifford, A. A., Duckels, M. I., and Walker, B. "Reflectance Phase-Shift Dispersion Relation." *Journal of the Chemical Society*, Faraday Transactions II, Vol. 68, No. 3, 1972, pp. 407-412.

35. Plaskett, J. S. and Schatz, P. N. "On the Robinson and Price (Kramers-Kronig) Method of Interpreting Reflection Data Taken through a Transparent Window." *The Journal of Chemical Physics*, Vol. 38, No. 3, 1 February 1963, pp. 612-617.

36. Jenkins, F. A. and White, H. E. *Fundamentals of Optics*, McGraw-Hill Book Company, New York, 1976, 4th Ed.

37. Born, J. and Wolf, E. *Principles of Optics*, Pergamon Press, Oxford, 1975, 5th Ed.

38. Palmer, K. F. and Williams, M. Z. "An Investigation of the Techniques of Ellipsometry, Internal Reflection, Reflection Spectroscopy and Moment Analysis to the Study of Films and Substrates." AEDC-TR-80-51 (AD-A093930), January 1981.

39. Miloslavskii, V. K. "Use of the Kramers-Kronig Integral Relations for Determining the Optical Constants of Metals in a Limited Spectral Region." *Optica i Spektroskopiya*, Vol. 21, No. 3, September 1966, pp. 343-346. (*Optics and Spectroscopy*, Vol. 21, No. 3, September 1966, pp. 193-195.)

40. Bennett, H. E., Silver, M., and Ashley, E. J. "Infrared Reflectance of Aluminum Evaporated in Ultra-High Vacuum." *Journal of the Optical Society of America*, Vol. 53, No. 9, September 1963, pp. 1089-1095.

41. Shklyarevskii, I. N. and Yarovaya, R. G. "Quantum Absorption in Aluminum and Indium." *Optica i Spektroskopiya*, Vol. 16, No. 1, January 1964, pp. 85-91. (*Optics and Spectroscopy*, Vol. 16, No. 1, January 1964, pp. 45-48.)

42. Golovashkin, A. I., Motulevich, G. P., and Shubin, A. A. "Determination of Microscopic Parameters of Aluminum from Its Optical Constants and Electrical Conductivity." *Zh. Eksperim. i Teor. Fiz.*, Vol. 38, January 1960, pp. 51-55. (*Soviet Physics JETP*, Vol. 11, No. 1, July 1960, pp. 38-41.)

43. Landau, L. D. and Lifshitz, E. M. *Statistical Physics*, Addison-Wesley Publishing Company, Reading, Massachusetts, 1969, 2nd Ed.

44. Toll, J. S. "Causality and the Dispersion Relations: Logical Foundations." *Physical Revue*, Vol. 104, No. 4, 15 December 1956, pp. 1760-1770.

45. Kreyszig, E. *Advanced Engineering Mathematics*, John Wiley and Sons, Inc., New York, 1967, 2nd Ed.

46. Smith, D. Y. "Dispersion Relations for Complex Reflectivities." *Journal of the Optical Society of America*, Vol. 67, No. 4, April 1977, pp. 570-571.

47. Fogel, M., Director. *Handbook of Formulas, Tables, Functions, Graphs, Transforms.* Research and Education Association, New York, p. 192, 1980.

48. Kittel, C. *Introduction to Solid State Physics*, John Wiley and Sons, Inc., New York, 1966, 3rd Ed.

49. Huber, E. D. "Extrapolated Least-Squares Optimization: A New Approach to Least-Squares Optimization in Optical Design." *Applied Optics*, Vol. 20, No. 10, May 1982, pp. 1705-1707.